School of Biomedical Engineering

Faculty of Engineering

The University of New South Wales

Computational and Experimental Assessment of the Mechanical Performance of Stents

Author: Anushan Senthurnathan

Submitted: 11 May 2020 Student zID: z5076499
Supervisor: Dr Susann Beier (UNSW)

Abstract

Cardiovascular disease treatments have been revolutionised with the introduction of stenting techniques being developed and improved over the years. This study aims to investigate methods both computationally and experimentally that can be used to evaluate the mechanical performance of stents. The computational objectives of the research was to design simulations to assess longitudinal compression, flexibility and radial strength of various stent designs. The experimental studies aim to analyse the compressive strength and deliverability of stents. This study aims to assist in evaluating the structural integrity of stent's to reduce mechanical failure and improve clinical outcomes.

The computational studies were designed using ANSYS commercial software and validated using research literature. The compression study agreed well with literature, especially for smaller forces applied (< 0.2 N with < ±0.25mm difference). The bending simulation agreed well with research literature, with less than a ±0.05mm (1.1%) difference and the radial strength simulation show good correlation for compression behaviour when smaller forces were applied (< 1.2 N with < ±0.06mm difference).

The compression and bending simulations then tested 18 stents which were previously found to be hemodynamically ideal, for their mechanical performance. These stent designs used seven major design variables, including: stent cross-sectional shape, stent dimension, strut angle, alignment type, cell height, connector type and number of connectors. The results found majority of the stents showed a considerably weaker compressive stiffness (<0.05 N/mm) and bending stiffness (0.074-1.86 N/mm^2) compared to commercial stents compressive (0.16-0.53 N/mm) and bending stiffness's (0.62-8.65 N/mm^2). The study determined circular cross-sections are superior in bending flexibility and are equally or even stronger in their compressive stiffness compared to rectangular cross-sections. Furthermore, a material comparison study conducted on the computational simulations found that Cobalt Chromium provided greater compressive strength and Magnesium alloy allowed for increased bending flexibility.

The experimental studies objectives also focused on assessing mechanical performance. The compression and deliverability experiment has proven to have conceptual design that can effectively test the mechanical performance. Feedback from academics and surgeons have been evaluated to improve the design setup and constraints to better evaluate stent mechanical performance. By considering the results gathered during this project both computationally and experimentally, it is evident that utilising an effective methodology that has been validated to test different mechanical parameters has potential to reveal meaningful insights into design characteristics.

Acknowledgement

Firstly, I would like to express my gratitude to Dr Susann Beier for overseeing the progress of my thesis work, for her guidance, assistance, constructive critiques and support over the entire year. I have learnt so much from her guidance over the course of this research project and her vast knowledge was essential to the completion of this thesis. I would like to thank Ramtin Gharleghi, Somesh Khullar and Jinbo Liu, for their time and assistance troubleshooting problems and getting acquainted with software resources. I would also like to thank Dr Ray Taprabata for his expertise in multi-objective optimisation and Dr Gangadhara Prusty for his professional expertise on the mechanical performance of stent geometries. In addition, I would like to thank Nigel Jepson and Kiran Sarathy for their surgical input on the experimental studies.

This research project was completed using assistance from services provided by the National Computational Infrastructure (NCI) and katana, a shared computational cluster located on campus at UNSW. I would like to extend my thanks for their continuous support in a timely manner to my requests for help.

Table of Contents

Abstract ii
Acknowledgement iii
List of Figures vi
List of Tables vii
Nomenclature viii
Chapter 1 - Introduction 1
1.1 Coronary stents for treatment of cardiovascular diseases 1
1.2 Stent Design 2
1.2.1 Stent Geometry Types 2
1.2.2 Expansion Mechanism 3
1.2.3 Material Composition 3
1.3 Finite Element Analysis 3
1.4 Mechanical Failure of Stents 4
1.4.1 In-stent Restenosis 4
1.4.2 Statistics on Stent Failure 5
1.5 Importance of Mechanical Integrity for Failure Prevention 6
Chapter 2 – Literature Review 8
2.1 Importance of Longitudinal Strength and Bending Flexibility 8
2.2 Geometric Parameters effect on Mechanical Characteristics 8
2.2.1 Cross-sectional shape 9
2.2.2 Strut Thickness 10
2.2.3 Connector Geometry 10
2.2.4 Connector and Hoop Alignment 11
2.2.5 Strut Amplitude and Curvature Radius of Sinusoidal Hoop 11
2.3 Implicit Finite Element Method 12
2.4 Computational Modelling 13
2.4.1 Numerical Model 13
2.4.2 Meshing Structure 13
2.4.3 Material Properties 13
2.4.4 Boundary Conditions 14
2.5 Motivation for Research 15
Chapter 3 - Methodology 16
3.1 Mechanical Research Objective 16
3.2 Computational Methodology 17

3.2.1 Stent Geometric Model 17
3.2.2 Design constraints 17
3.2.3 Computational Simulation 18
3.3 Material Performance Comparison 25
3.4 Deliverability Experimental Protocol 25
3.4.1 Aim: 25
3.4.2 Objectives: 25
3.4.3 Apparatus: 25
3.4.4 Experimental Setup: 26
3.4.5 Method: 26
3.3.6 Analysis: 26
3.5 Compression Experimental Protocol 26
3.5.1 Aim: 26
3.5.2 Objectives: 26
3.5.3 Materials: 26
3.5.4 Experimental Setup: 27
3.5.5 Method: 27
3.5.6 Analysis: 27
Chapter 4 – Results 28
4.1 Validation of Simulations 28
4.2 Mechanical Integrity Assessment 30
4.3 Initial Sample Performance 31
4.4 Material Comparison Simulations 32
4.5 Research Opportunity and Performance Evidence (ROPE) 33
Chapter 5 – Discussion 34
Chapter 6 – Conclusion 39
References 40
Appendix A – Delivery Experiment 43
Appendix B – Deliverability Experiment Questionnaire 44
Appendix C – Commercial Stents Comparison 45

List of Figures

Figure 1: Diagram of Angioplasty and Stent Implantation Process [5] 2
Figure 2: Coronary Stent Technical Requirements [6] 2
Figure 3: Factors Influencing the Development of In-stent Restenosis [11] 5
Figure 4: Mechanical forces and deformation that can occur to an artery [8] 6
Figure 5: Commercial Designs for Coronary Stents [18] 9
Figure 6: Cross-sectional Shape Examples 9
Figure 7: Different types of connectors 11
Figure 8: Diagram of strut amplitude and curvature 11
Figure 9: Effect of amplitude on longitudinal strength (RHS), Effect of curvature radius on longitudinal strength (LHS) [23] 12
Figure 10: Example of a compression Bench testing for stents [31] 14
Figure 11: Bending Flexibility Boundary Conditions 14
Figure 12: Types of radial strength simulations 15
Figure 13: Design Variables 18
Figure 14: LHS meshing for compression validation simulation, RHS meshing for bending flexibility validation simulation 18
Figure 15: Compression Convergence Study 19
Figure 16: Bending convergence study 20
Figure 17: Compression Study Boundary Conditions 20
Figure 18: Bending Simulation Boundary Conditions 21
Figure 19: Radial Test Boundary Conditions 21
Figure 20: Results for compression validation simulation 22
Figure 21: Hooke's Law limit in elastic region 22
Figure 22: Results for bending flexibility validation simulation 23
Figure 23: Before and after versions of radially compressed stent ring 23
Figure 24: Young's Modulus chart [38] 24
Figure 25: Experimental setup 26
Figure 26: Compression Experiment Setup 27
Figure 27: Compression Strength of Omega Stent 28
Figure 28: Validation on Bending Flexibility 29
Figure 29: RHS Radial Strength Simulation comparison, LHS Simulation results zoomed in on the Elastic region of material 30
Figure 30: Compressive stiffness vs bending stiffness (with stent 16) 31
Figure 31: Compressive stiffness vs bending stiffness (without stent 16) 32
Figure 32: Circular and rectangular cross-section comparison 34
Figure 33: Mechanical performance of connectors 35
Figure 34: Material stiffness comparison 36
Figure 35: Deliverability experimental work 36
Figure 36: LHS system setup in sections, RHS a stent delivery system in solid gel 37

List of Tables

Table 1: Statistics on Stent Failure [7] 6
Table 2: Material Properties of Platinum Chromium Alloy [29] 13
Table 3: Design Variables and Design Constraints 17
Table 4: Material Properties 25
Table 5: Mechanical analysis of hemodynamically optimised stents 30
Table 6: Material comparison for stents 32
Table 7: Mechanical performance comparison with commercial stents 35
Table 8: Delivery Experiment radius of curvature at each junction 43
Table 9: Compressive stiffness commercial stent comparison 45
Table 10: Bending flexibility commercial stent comparison 45

Nomenclature

Abbreviation	Definition
$\mathbf{P_{cr}}$	Critical force
E	Elastic modulus
I	Area moment of inertia
K	Column effective length factor
L	Length
M	Moment equation for beam
y	Vertical Displacement
Δu	Increment of displacement
$\mathbf{K_t}$	The current tangent stiffness matrix
F	Applied load vector
I	Internal force vector
M	Mass matrix
K	Stiffness matrix
u	Displacement vector
k	Compressive Stiffness
x	Deflection
f	Bending Deflection

Chapter 1 - Introduction

1.1 Coronary stents for treatment of cardiovascular diseases

Cardiovascular disease treatments have been revolutionised with the introduction of coronary angioplasty and stenting techniques being developed over the years. One of the leading causes of mortality and morbidity around the world is caused by coronary artery diseases[1]. Coronary vascular diseases can be caused by atherosclerosis, syphilis, congenital defects, hereditary conditions and health problems caused by factors such as obesity and smoking. Cardiovascular diseases that cause a narrowing of the arterial vessel walls or involve an accumulation and build-up of cells, lipids, connective tissue, calcium, and other substances along the arterial wall, can restrict the healthy flow of blood to all areas of the body including the heart[2].

A procedure involving balloon angioplasty and stent implantation is often implemented in order to restore healthy blood flow to vessels. In 1964, Dotter and Judkins used implantable prosthetic device to conceptually describe the concept of angioplasty, and then in 1977 during bypass graft surgery, Andreas Gruntzig performed the first coronary angioplasty. During the 1980s the concept of stents was developed and was first implemented as a form of treatment in 1986 by Sigwart and Puel. Since then the coronary stent has been further developed focusing primarily on design refinement and material composition [1].

Stenosis can be treated using three different methods, including: endovascular intervention, pharmaceutical drugs and surgically. Drug treatment has been known to only reduce the relative risk caused by stenosis by 13% and also requires numerous dosage cycles and can have side effects. The surgical procedure has a high mortality and morbidity due to surgical complications and permanent harm to patients caused during operations[3]. Amongst the medical community endovascular intervention treatment has grown in popularity since its inception, as it has transformed the means of alleviating arterial narrowing and stenosis through the use of stents structures. Coronary stents provide vessel scaffolding and have a mesh tube structure to hold the vessel wall in position. Even with advancements in stent design the adverse clinical outcomes of stent implantation is about 10%. The percutaneous coronary intervention process for implanting stents continues to be studied and refined in order to optimize the design and reduce the risk of failure[4].

The percutaneous coronary intervention (PCI) is the treatment of implanting a stent into a blood vessel through angioplasty. This is an invasive procedure where a collapsed balloon and stent catheter is guided to an area within a blood vessel that is experiencing stenosis. Once the catheter is correctly positioned the balloon expands widening the lumen of the vessel, and ultimately increasing the blood flow. Angioplasty was originally a treatment option, although it only provided a temporary fix as the vessel would often close after a few days or weeks. To overcome this issue an expandable mesh structured stent was designed in order to remain in the vessel and prevent further narrowing. Overall coronary stents have been considered to be effective treatment options due to their high success rate, long term management of the vessel and lesser invasive surgical procedure[5].

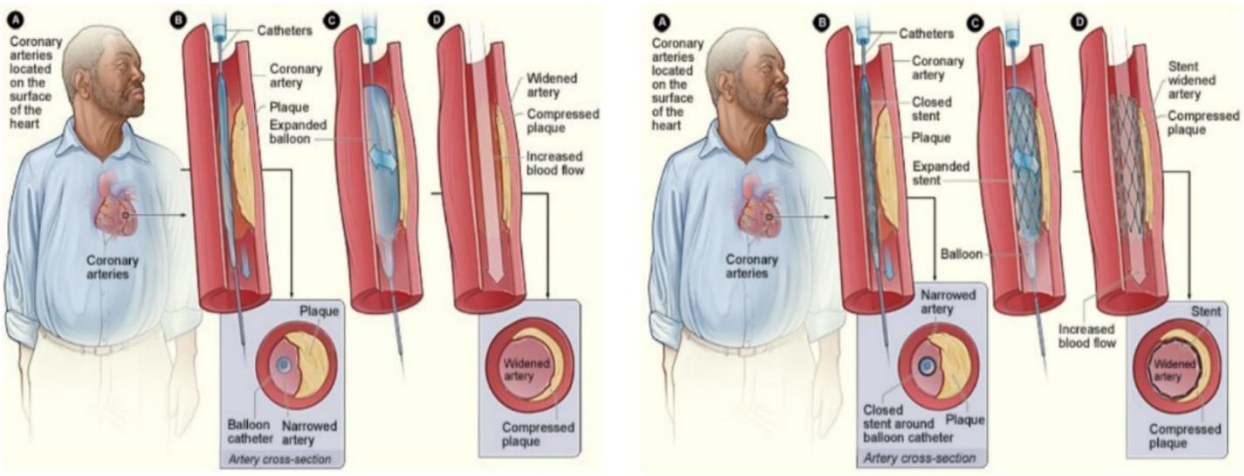

Figure 1: Diagram of Angioplasty and Stent Implantation Process [5]

1.2 Stent Design

The ideal stent design must comply with medical standards, be biocompatible with the vessel and satisfy a broad range of technical requirements. The ideal coronary stent design needs to be comprised of many desirable characteristics, although the advancement of one aspect can have a deteriorating effect on another aspect. The diagram below demonstrates some of the major design considerations that are investigated for stent design and displays the effect of varying different design parameters[6].

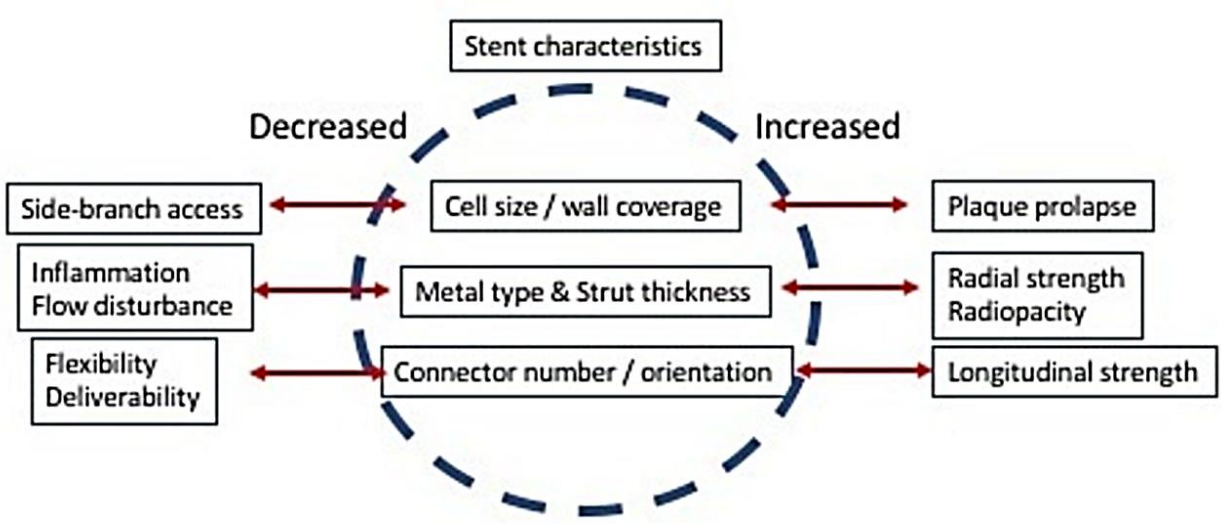

Figure 2: Coronary Stent Technical Requirements [6]

1.2.1 Stent Geometry Types

Stents can be categorised into two groups, closed-cell and open cell designs. Closed cell design stents have connector elements on each strut of the sinusoidal ring, compared to an open cell design which has connector struts and sinusoidal rings selectively joined. The connector struts come in various shape, the most common design is sinusoidal, straight or Z-shaped[7]. There are also various types of stents, each having their specific benefits. The most common types include: bare-metal stents, drug-eluting stent and biodegradable stents.

Bare-metal stents – The original design for the stent with a mesh structure used to hold the vascular walls in place to prevent stenosis. Bare-metal stents have good long term effectiveness, reduces restenosis and has a strong success rate[8].

Drug-eluting stents – The geometry of the stent is similar to the bare-metal stent, although it has a slow releasing drug coating. The stent is primarily placed in diseased peripheral and coronary arteries in areas of stenosis in order to reduce cell proliferation and heal the traumatized areas[8].

Biodegradable/ Bioresorbable Stents – These stents also have similar geometries. The main difference is the material composition is designed to be reabsorbed by the body in a time frame from three months to two years[8].

1.2.2 Expansion Mechanism

The expansion method for a coronary stent can either be balloon expandable or self-expandable. A self-expanding stent are made of shape memory alloy, which allows the stent to plastically deform in shape when the stent is below critical temperature and then revert back to the original shape once heated. The balloon expandable stents are designed to be manufactured in their operational geometries and are then crimped onto the angioplasty balloon. Once the balloon expands the stent reverts back to its original shape[7]. The mechanism must be flexible and well designed in order to facilitate deliverability to areas of stenosis.

1.2.3 Material Composition

The material composition for the stents need to have strong corrosive resistance, be biocompatible with the surrounding environment and good radio opacity. Radio opacity refers to the stent having minimal interference with Magnetic Resonance Imaging. For balloon expandable stents Cobalt Chromium is the most common material, although different alloy combinations are gradually becoming more popular. The self-expanding stent requires a material that can perform shape memory and at the moment Nitinol is the most common material selection. The first generation of bioresorbable stents are often manufactured using Poly-L-Lactid Acid (PLLA) or Magnesium alloys. In general the material selection is based on the materials suitability for optimal performance[7].

1.3 Finite Element Analysis

Computational simulations are often used in design processes as they provide useful methods for evaluating various real world scenarios in order to determine if the mechanical structures of designs are appropriate for their function. When investigating various stent designs finite element analysis (FEA) of the model provide useful insights into the stents potential performance before manufacturing the product. The computational studies along with practical experiments provide important data which can be used to further improve and optimize the design for various vessel conditions. In order to further improve the final outcome of the stent geometry, finite element analysis provides a cost effective method of estimating mechanical behaviour of stents for situations including reaction to implantation or the impact of arterial wall stress on the structure[5].

Finite element analysis provides a method of computationally studying the mechanical behaviour of stents in order to determine which aspects and parameters influence success and failures in design. The biomechanical attributes of stents are evaluated using this computer based method as a pre-clinical testing tool. The numerical method used to solve the simulations depends on the geometric input, the various loading conditions, the material properties of the model and the boundary conditions. The simulation endeavours to mathematically describe the behaviour of the stent model by separating the stent geometry into a finite number of discrete regions. The nodes and elements is then solved to provide an approximate solution for the entire stent model. The process of deriving various mechanical behaviours such as displacement, strain and stress, all rely on each other for calculating values. Once the simulation has been appropriately setup, the displacement at any point on the model is derived by interpolating the nodal displacements in the element. Then by using the appropriate derivatives of the displacement the strain can be deduced for the element at any point. The material properties of the model are then used to provide a basis for the calculation for the stress using the strain values. In general finite element analysis is able to create equations of discrete nodal quantities from input variables to solve for various parameters. Finite element analysis has the capability of providing exact physical solutions under the assumption that appropriate numerical requirements and accurate modular setup are satisfied[9].

In terms of design optimization finite element analysis is used by medical device manufacturers in order to predict biomechanical solutions. However, there are limitations to FEA that can affect the geometric accuracy of the approximated solution. FEA is limited by the mesh density, as to accurately solve complex geometries an extremely refined mesh with a high number of elements is required. This is due to the continuum domain being discretised using low-order and low-regularity polynomials. There are various techniques that can be implemented to refine a mesh geometry, although the larger the number of elements and nodes the greater the computational time and computational power are required. FEA is limited by the basis function, as it prevents the system from appropriately approximating the solution without requiring a high number of degrees of freedom. There is also limitation in the accuracy of the solution as there is an accumulation on computational error that increases with every calculation. Although there are limitations to finite element analysis, they can all be managed by creating suitable geometric designs and simulation setups[10].

1.4 Mechanical Failure of Stents

1.4.1 In-stent Restenosis

The mechanical failure in stents is due restenosis that occurs post-implantation of the stent. After the deployment of the stent, the ratio of restenosis has reduced from 33-55% to 15-20% when compared to normal balloon angioplasty treatment. In-stent restenosis is the narrowing of the vessels wall in reaction to the stent post procedure and is the main cause of mechanical failure[5]. There are five main categories that influence the development of restenosis post stent implantation. Figure 3 below visual displays the main aspects of each category effecting restenosis. Amongst this list of influences the factor that has the most impact on in-stent restenosis is lesion characteristics[11].

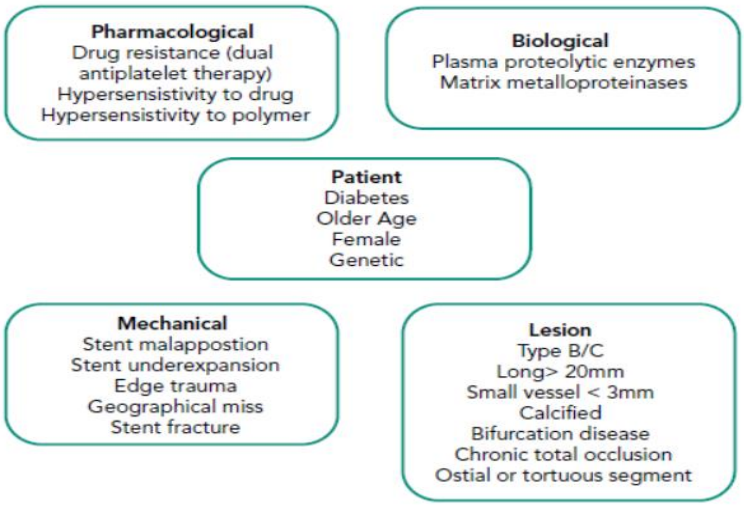

Figure 3: Factors Influencing the Development of In-stent Restenosis [11]

Most reoccurrences of stenosis are due to arterial injury or inflammatory response of the vessel wall. The aspects that contribute to the post-stenting narrowing can include:[10]

i. Immediate narrowing of the lumen can occur due to excessive stent elastic recoil.
ii. Injuries to the vessel wall caused due to stent expansion, stent recoil or damage during vessel movement.
iii. Stresses generated in the tissue of the vessel can cause remodelling, which may involve restenosis.

These responses can result in an abnormal growth in endothelial cells in the effected region. These reactions are known as stent thrombosis and neointimal hyperplasia. Stent thrombosis is the formation of blood clotting around the stent due to injury to the vessel wall. Neointimal hyperplasia is a growth in cells around the stent usually due to aggressive technique during balloon and stent expansion causing arterial injury and inflammatory reactions. There are also various other factors that can cause stent failure, such as: under expanding stents, inappropriately sized stent and lesions[5].

1.4.2 Statistics on Stent Failure

There have been many clinical studies that have been performed in order to understand the statistical chance of stent failure. These studies gather data over a large basis and determine the frequency and percentage of occurrences where stents have failed. Schiavone et al. (2015) has collected various case studies in order to determine the causes and number of occurrences of failure within a controlled group. The data has been summarized in the table below[7].

Table 1: Statistics on Stent Failure [7]

Context of Case Study	*Number of Patients*	*Reason for Stent Failure*	*Percentage of Failure*
Determine the number of stent failures due to fracture according to the guidelines of American College of Cardiology-American Heart Association	415	Minor, moderate and severe fracture	1.7%
Stent Failure after 6 month period	199 patients treated with serolimus eluting stents,	Thrombosis due to stent fracture after 6 months	1%
Stent failure after (14±9) months of deployment where patients underwent follow-up coronary angiography	868 patients	66 patients underwent follow-up coronary angiography. The follow-up showed 26 with lesions of which 10 had stent fractures.	3% - problems 1.15% - stent fracture
Stent fracture study	422 patients	33 patients had stent fractures of which 18 had complete fracture.	7.7% - stent fracture 4.2% - complete stent fracture

These case studies ran from 2007 to 2009. Over the years the stent design has been developed to have less risk of fracturing and harming the patient. Stent fracture, stent collapse and arterial wall damage are the primary contributors to health complications for a patient [7]. Overall considering every possible method of failure for stents approximately 10% fail, which is significantly high considering the millions of procedures performed yearly[4].

1.5 Importance of Mechanical Integrity for Failure Prevention

There is a great deal of importance in generating a stent design that has strong mechanical integrity as majority of stent failures are fractures in the structure. These fractures cause damage to the arterial wall causing scar tissue proliferation, stent thrombosis and neointimal hyperplasia. Stent designs experience various mechanical force within an arterial vessel demonstrated in the figure below.

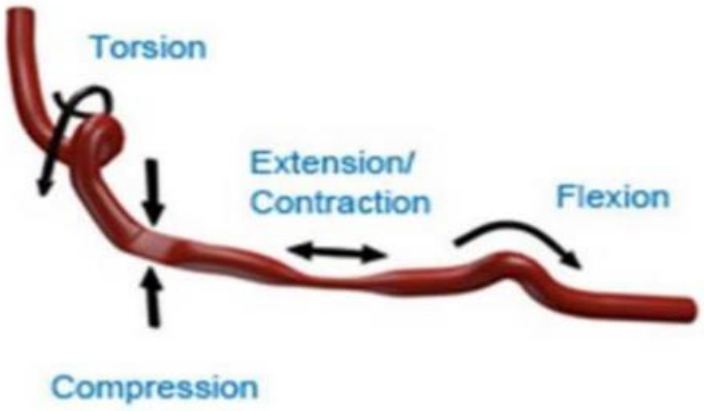

Figure 4: Mechanical forces and deformation that can occur to an artery [8]

The optimal stent design endeavours to exemplify the following characteristics: [10]

i. Guarantee good flexibility to ensure an efficient and safe deployment of the stent during surgery and allow for stent conformability post implantation.
ii. Offer suitable radial and longitudinal strength to minimize the elastic recoil, vessel injury due to stent assembly and prevent fracture in structure.
iii. Provide a strong dense mesh structure to reduce tissue prolapse.

These characteristics are often sought after, but as demonstrated in Figure 2 optimising one mechanical parameter can deteriorate another. In order to improve the flexibility and decrease metal to artery ratio, a reduction in connectors is desirable, although this negatively effects the longitudinal strength. Overall establishing a balance between the numerous mechanical properties is an important parameter to consider when reducing the risk of failure due to coronary stent design[12].

Chapter 2 – Literature Review

This chapter provides a review of current literature with relevance to the longitudinal strength and bending flexibility of a coronary stent.

2.1 Importance of Longitudinal Strength and Bending Flexibility

The ideal stent design must fulfil a range of technical requirements in order to effectively elevate narrowing sections of blood vessels without structural failure. The longitudinal integrity of stents has been given less attention in terms of research and optimisation. Current research into stent geometry focuses on radial strength, deliverability and conformability, which has a negative effect on the longitudinal integrity of the stent structure. The longitudinal integrity of coronary stents have been found to have a strong correlation with the connector design, alignment and positioning between hoops as well as the strength of the stent hoops[6].

The bending flexibility of stents is an integral design consideration as cardiac contractions and relaxations can cause bending angles that can affect the structure of the stent. Minimal research has been conducted so far on the relationship between fractures and bending motions[13]. Flexibility enables to stent to change shape to follow vessel contours and reduce the distortion at the junction of the bend. The flexible characteristic allows for conformability when delivering the stent to the ideal location and its importance increases as the stent length increases. It is important to find a balance for the flexibility of stents as flexible stents can cause more plaque prolapse, recoil and increase subacute thrombosis[14].

Although infrequent, stent longitudinal distortion can lead to severe health problems and damage to the vessel wall. A study was performed by Hiromasa et al. investigated the clinical impact of longitudinal stent deformation after implantation. The case study involved 809 patients with 1052 lesions and found that longitudinal strength deformation after implantation occurs in approximately 1.9% of lesions[15]. Another case study investigated the deployment of 1,000 stents and determined stent failure due to major deformation in structure in 1.8% of the cases. From these nine cases required re-stenting and major adverse cardiac events occurred in five cases[16]. Longitudinal stent deformation can be caused by several mechanisms including: post-dilatation balloons, guide catheter extensions and proximal embolic protection devices. It is important to identify when major stent deformation occurs as if left untreated can cause major adverse cardiac events or stent thrombosis[17].

2.2 Geometric Parameters effect on Mechanical Characteristics

There are significant variations between commercial stent designs on the market. The variations in the geometric parameters have been known to change the performance of the stent as indicated in Figure 2. The primary design variables for stents that affect the mechanical strength include: strut cross-sectional shape, strut thickness, connector geometry and strut alignment. These factors influence the longitudinal integrity of the coronary stent and are considered to be the most relevant factors when influencing the design. Figure 5 below displays some possible geometric designs for coronary stent that are currently commercially available. This figure also demonstrates the immense differences present in current stent geometric designs.

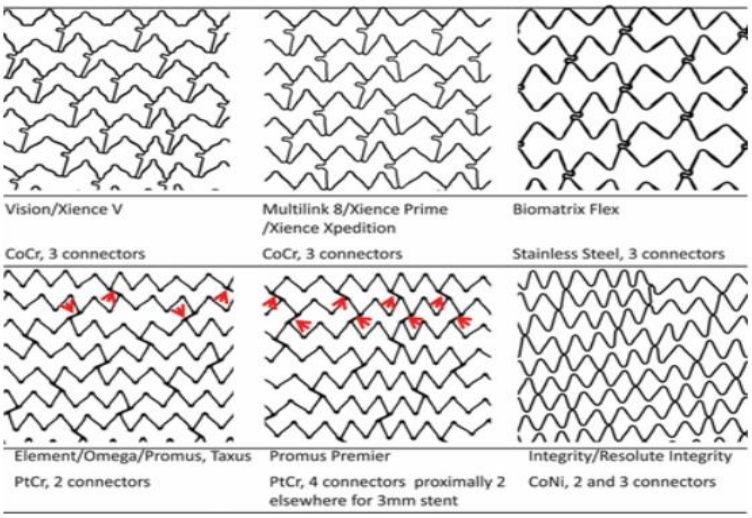

Figure 5: Commercial Designs for Coronary Stents [18]

2.2.1 Cross-sectional shape

The cross-sectional shape of the struts causes changes to the amount of force the stent structure can support without fracturing. The cross-sectional geometry can vary between: circular, square, rectangular, triangular and irregular shapes[19]. Figure 6 displays some cross-sectional shapes for struts that were considered for this project.

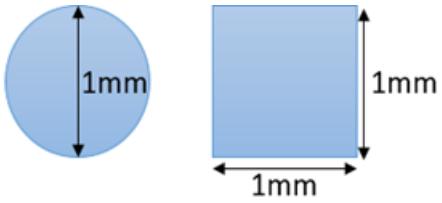

Figure 6: Cross-sectional Shape Examples

Investigating the mechanical characteristics of the struts as beam structures can demonstrate how different cross-sectional shapes effect the structural integrity. Buckling and deflection due to bending are the main causes of mechanical failure for stents in terms of longitudinal integrity. The formula for buckling can be represented as: [20]

$$P_{cr} = \frac{\pi^2 EI}{(KL)^2}$$

The deflection due to bending can be represented as:

$$y = \frac{1}{EI} \iint M\, dx$$

The moment of inertia (I) for the circle and square shape shown in Figure 6 are 0.04909 mm^4 and 0.08333 mm^4, respectively. If the assumption is made that all other parameters for the sturts were the same, the maximum critical force allowed before buckling and the deflection due to bending can be derived to be: [21]

$$P_{cr,circle} = 0.04909 P_{cr}, \qquad P_{cr,square} = 0.08333 P_{cr}$$

$$y_{circle} = 20.371 y, y_{square} = 12.000 y$$

After investigating the values presented, it can be determined that square shaped cross-sections provide greater structural strength. The square cross-sectional shape can handle a larger applied force before buckling and has less deflection due to bending. Although the square shape demonstrates good structural strength, it does have sharp edges. Those sharp sections are more susceptible to fracturing due to being areas of great stress during bending. These calculations are limited as they are derived for straight beams, but the principle is similar for curve beams. In general these theoretical calculations demonstrate the importance and impact of cross-sectional shape of the longitudinal integrity of stents[21].

2.2.2 Strut Thickness

The strut thickness is one of the primary determinants of mechanical strength for stent structures. The strut thickness is important for maintaining the appropriate level of radio-opacity, longitudinal and radial strength. 316L Stainless Steel material was used in manufacturing first generation stents and has recently started being replaced by alloy materials like cobalt chrome and platinum chromium. Alloys have been introduced in order to reduce the strut thickness due to stronger material properties while maintaining effective performance. Lower strut thicknesses are preferred due to the reduction in disturbances of blood flow, improved deliverability of stent during implantation, decrease in abnormal shear parameters and reduction in localised inflammations caused during and post implantation[6].

A case study was performed involving 651 patients where a commercially available stent in two different sizes were implanted. The results found that the thinner stent had a 15.0% chance of angiographic restenosis and had a reduction in clinical restenosis with 8.6% requiring reintervention. Comparably the thicker stent had a 25.8% chance of angiographic restenosis and had cases of clinical restenosis with 13.8% requiring reintervention. The outcome of the study found that thinner strut stents provided a considerable reduction of angiographic and clinical restenosis after implantation [22].

2.2.3 Connector Geometry

The connector geometries are used to connect the hoops of the stent together and play an integral part in allowing flexible movement and longitudinal strength. Commercial stents often use connectors that are straight, S shaped or M shaped as shown in Figure 7. Studies have shown that the L-stent connector has the highest longitudinal stent strength while the S-stent has the lowest. The L-stent was found to be twice as strong in terms of longitudinal strength when compressing the stent 0.62mm[23].

When examining the mechanical structure of the connectors the straight connecter has a greater longitudinal stiffness and is able to provide greater resistance to compressive forces. The straight connector performance is superior as long as the force applied on each connector does not exceed the critical force allowed, which would cause the connector to fracture or buckle. The S-stent and M-stent have a spring structure, which allows them to handle a greater compressive force before fracture, but causes them to deform more easily. While these two stent types have lower longitudinal strength, they are able to handle a greater amount of force before permanent deformation. Additionally these stents can revert back to their original shape if the given forces are smaller than the critical force that would cause the material to surpass the yield stress, but the recoil of the stent can have damaging effects to the vessel.

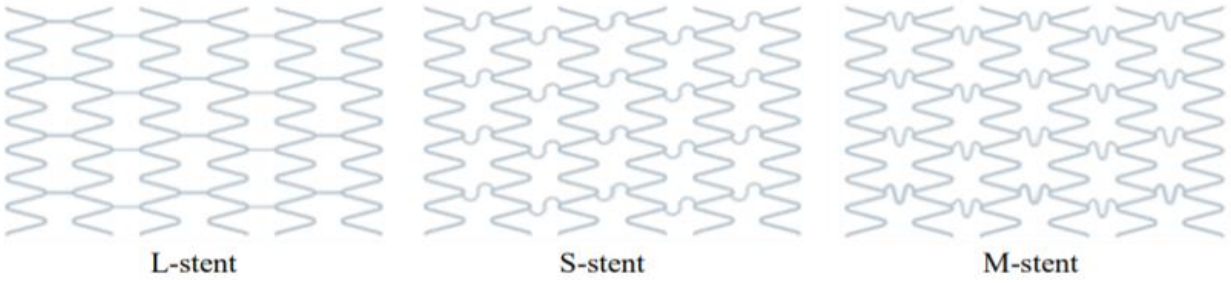

Figure 7: Different types of connectors

2.2.4 Connector and Hoop Alignment

The stent geometry consists of numerous sinusoidal hoops linked together with a specified connector type. Most modern models are usually designed with 1-3 connectors with the hoops being aligned in phase (peak to valley) or out of phase (peak to peak). The alignment is an integral component for longitudinal strength as connector can be aligned to form a strong spring structure or a stiff spine to optimize stent longitudinal integrity. Understandably alignment heavily impact the bending flexibility, for example the Cypher stent has six connectors between the hoops which can increase the longitudinal strength considerably, although reduce the bending flexibility significantly due to the stiffness of the structure[6].

A point compression study was performed on a set of commercially available stents and found that the hoops of the stents gets pushed together. Compression was greater on the side of the point source and lower on the opposite side. This study also found that the hoops would overlap, which would cause obstruction to the flow and the stent to protrude into the lumen and vessel wall[18]. Another study performed by Iwasaki et al. determined that the stent flexibility is higher for lower number of connectors when the stent is experiencing cyclical bending motions[13]. These studies further support the importance of longitudinal and bending flexibility in stent designs.

2.2.5 Strut Amplitude and Curvature Radius of Sinusoidal Hoop

Some other factors that are often varied to influence change in the stent performance is the strut amplitude and the sinusoidal hoop radius of curvature. Figure 8 visually shows the strut amplitude as the height of the sinusoidal hoop (*f*) and radius of curvature (ρ) as the curve at the peak and valley. These characteristics were investigated by Shen et al. where they compare various curvature diameters and amplitude heights. It was determined that the amplitude and curvature radius had limited effect on the longitudinal strength. Figure 9 graphically represents the results for changing these factors and demonstrates they have limited impact in terms of longitudinal integrity[23].

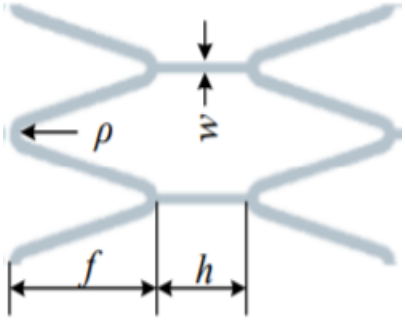

Figure 8: Diagram of strut amplitude and curvature

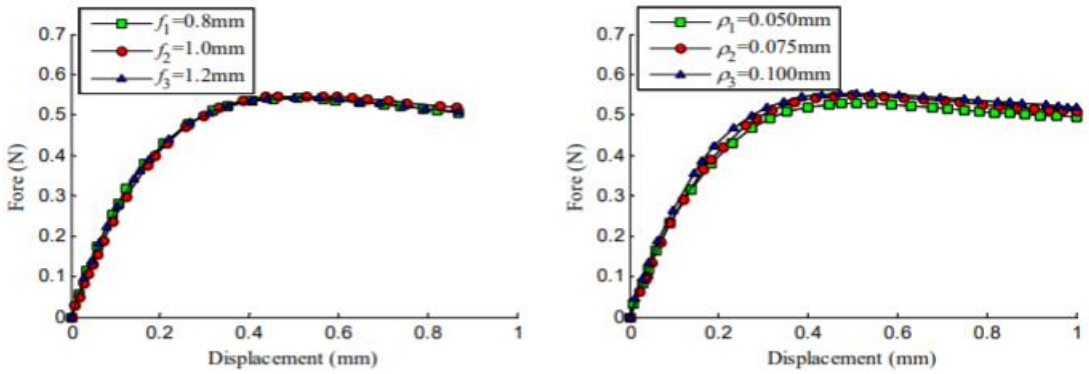

Figure 9: Effect of amplitude on longitudinal strength (RHS), Effect of curvature radius on longitudinal strength (LHS) [23]

2.3 Implicit Finite Element Method

Finite element analysis can provide insight into the performance and structural integrity of stent designs, while highlighting parameters that are sensitive or critical to the mechanical structure. The model complexity and simulation requirements are the major contributing factors when determining the appropriate numerical approach and computational platform. Implicit finite element method is often utilised in scenarios of low deformation rate and for simulations with simple boundary conditions. Implicit formulation is an effective method for solving equations associated with material nonlinearities involving hyperplastic materials that have displacement dependent properties and for explaining geometrical equation involving situations similar to deformation[24].

The computational static structural analysis of a stent involves a stiffness-based implicit method that implements the Newton iterative method based on an incremental strategy. The dynamic quantities are solved based on the values at a given time and the change in time. The implicit equation can be represent as follows:

$$\Delta \boldsymbol{u}_{\boldsymbol{i+1}} = \Delta \boldsymbol{u}_{\boldsymbol{i}} + \boldsymbol{K}_{\boldsymbol{t}}^{-\mathbf{1}} \times (\boldsymbol{F}_{\boldsymbol{i}} - \boldsymbol{I}_{\boldsymbol{i}})$$

Then the implicit dynamic procedure can be defined by the following algorithm:

$$\boldsymbol{M}\ddot{\mathrm{u}}_{\boldsymbol{i+1}} + (\mathbf{1} + \boldsymbol{\alpha})\boldsymbol{K}\boldsymbol{u}_{\boldsymbol{i+1}} - \boldsymbol{\alpha}\boldsymbol{K}\boldsymbol{u}_{\boldsymbol{i}} = \boldsymbol{F}_{\boldsymbol{i+1}}$$

Then the displacement and velocity vector can be derived:

$$\boldsymbol{u}_{\boldsymbol{i+1}} = \boldsymbol{u}_{\boldsymbol{i}} + \Delta \boldsymbol{t}\dot{\boldsymbol{u}}_{\boldsymbol{t}} + \Delta \boldsymbol{t}^{\mathbf{2}}\left[\left(\frac{\mathbf{1}}{\mathbf{2}} - \boldsymbol{\beta}\right)\ddot{\boldsymbol{u}}_{\boldsymbol{i}} + \boldsymbol{\beta}\ddot{\boldsymbol{u}}_{\boldsymbol{i+1}}\right]$$

And,

$$\dot{\boldsymbol{u}}_{\boldsymbol{i+1}} = \dot{\boldsymbol{u}}_{\boldsymbol{i}} + \Delta \boldsymbol{t}[(\mathbf{1} - \boldsymbol{\gamma})\ddot{\boldsymbol{u}}_{\boldsymbol{i}} + \boldsymbol{\gamma}\ddot{\boldsymbol{u}}_{\boldsymbol{i+1}}]$$

The implicit equations should be solved for each time increment based on Newton's iterative method. The procedure for solving the implicit code is unconditionally stable and is an efficient method for deriving deformations in geometries. The limitation with this method is that for complex models shortened time increments are required in order to accurately solve the tangent stiffness matrix for each iteration. This inevitably increases the computational time required to solve the numerical simulation. The addition of contact constraints increases the complexity of the model for the implicit code to solve, although doesn't affect the number of equations being deciphered[24].

2.4 Computational Modelling

Computation simulations are an effective and efficient method of examining mechanical characteristics of coronary stents experiencing various loading conditions. The stent geometry and boundary conditions are critical for accurately simulating appropriate conditions. Numerical studies focusing on structural integrity focus on model accuracy, geometric meshing, material properties and boundary conditions. The following section provides details on important aspects for each component.

2.4.1 Numerical Model

The numerical model aims to create an appropriate geometry that can represent real world scenarios. The mechanical properties of the stent can be examined by running simulation on the geometric model of the stent. In order to validate the simulation an appropriate model must be developed of commercial stent designs in order to compare with experimental data[25]. The stent geometric designs must resemble suitable structures in order to the optimized design to be used for clinical applications.

2.4.2 Meshing Structure

The numerical solution is solved by deriving values for each meshing element that has be discretised in the finite model. The meshing selection for the model is reliant on the complexity of the geometry. Previous studies on stent structure conducted the meshing using linear hexahedrons elements in order to reduce integrated elements[26]. In addition, grid sizing on the providing a layered thickness for the wall of the stent should be analysed in order to determine a suitable discretisation. The arrangement of the mesh should aim to have a cube structure to accurately determine the changes in geometry due to applied loading conditions[27]. To supplement the quality of the mesh a convergence study should be performed for the simulations in order to generate an appropriate balance between the accuracy of the solution and the computational time.

2.4.3 Material Properties

The material properties of the stent have a considerable impact on the geometry, primarily impacting the stent strut thickness. Previously 316L stainless steel was used to stent material, although recently alloys have been considered to be more effective. Alloys such as platinum chromium (PtCr) and cobalt chromium (CoCr) have been developed to provide a stronger structural strength and flexibility with less material. This reduction in the stent struts improves the deliverability, procedural outcome and reduces the rate of restenosis[28]. Platinum chromium has a high biocompatibility and mechanical strength, hence the numerical simulations for optimising the longitudinal strength of coronary stents was based on the mechanical properties of the alloy[29].

Table 2: Material Properties of Platinum Chromium Alloy [29]

Material Properties	***Magnitude***
Young's modulus [MPa]	203 000
Poisson ratio	0.285
Density [Kg/m^3]	7850
Tensile strength [MPa]	834
Yield point [MPa]	480

2.4.4 Boundary Conditions

2.4.4.1 Compression Simulation

The compression study to investigate the longitudinal compressive strength of the stent geometry can be performed using both symmetrical and point loading. In order to determine the overall strength of the stent symmetrical loading cases are preferred. To allow for a deep investigation multiple compression length should be experimented to replicate a range of clinical events[30]. Previous studies have performed the investigation by applying a symmetrical load on one side of the stent while the other end is fixed. This allows for a force-strain relationship analysis to take place, as vertical pressure is applied allowing for longitudinal deformation to be derived[31]. For numerical simulations the vertical loading can be increased incrementally in order to determine the deformation, point of permanent deformation and compressive stiffness of the stent. Figure 10 is an example of a bench testing setup for compressing a stent. Ideally the numerical simulations aim to replicate the conditions present in the experiment.

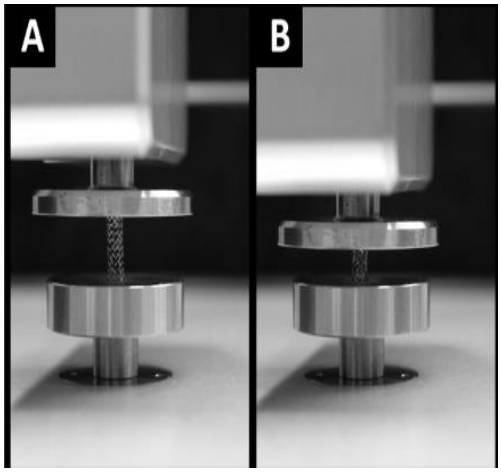

Figure 10: Example of a compression Bench testing for stents [31]

2.4.4.2 Bending Flexibility Simulation

The deflection in the stent cause by bending within a vessel can be analysed using a three point bending test. This involves having a stent rest on two static support structures while a load is applied to the middle. Figure 11 displays the general setup for a numerical simulation for investigating bending flexibility[32]. The load deflection relationship can determined by incrementally increasing the load to determine the bending stiffness of the stent. This numerical simulation can determine the deformation due to an applied load, the range of bending capabilities of the examined stent structure and the maximum bending force that can be applied before permanent deformation. The flexibility of the stent can be represented by the bending stiffness derived from the displacement and applied force[33].

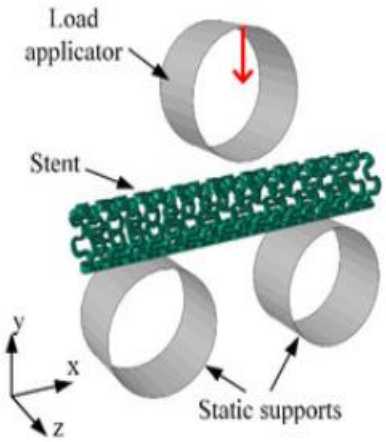

Figure 11: Bending Flexibility Boundary Conditions

2.4.4.3 Radial Strength Simulation

Computational models have been generated to examine the radial strength of stents. There are three main radial strength simulations that have been conducted in studies to evaluate the radial strength, which include:

- Applying a pressure force on the outside surface of a stent geometry to compress the stent radially.
- Constructing a stent geometry between two plates and then applying a load to the plates to compress the stent radially flattening the stent.

- Designing a cylindrical crimp on the outside of the stent. Then applying a displacement to the crimp to compress the stent in increments.

The load and deflection relationship can determined by incrementally increasing the load. This numerical simulation can determine the deformation due to an applied load and the maximum radial force that can be applied before permanent deformation or fracturing. The radial strength of the stent can be represented as a radial stiffness derived from the displacement and applied force[34].

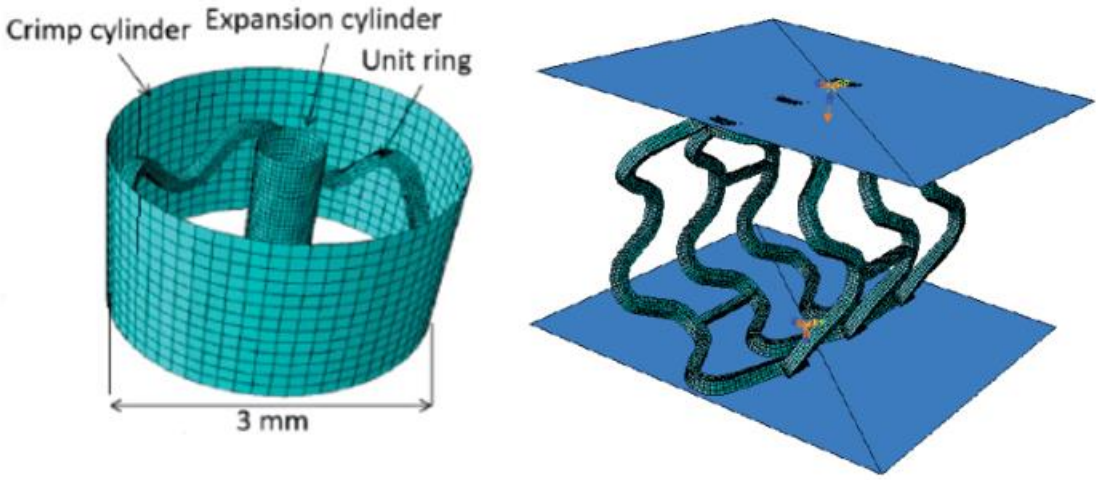

Figure 12: Types of radial strength simulations

2.5 Motivation for Research

The mechanical properties for coronary stents are important characteristics that can affect the performance of stents. After reviewing previous literature there is an apparent gap in research focusing on the optimisation of longitudinal strength, radial strength and flexibility. In addition, these factor are integral to the design as failure due to these characteristics causes deformation in the stents shape, which can cause injury to the patient and affect the hemodynamic flow of the stented artery. Previous studies aimed at investigating individual factors and haven't considered understanding mechanical design as an entire system. This provides a gap in knowledge in terms of the design of the stent as various variables affect the overall outcome and different combinations of design variables can create a stronger performance. Overall this research study focuses on identifying the influences of design variables on the structural integrity and aims to assess a range of designs for different geometric variables in order to help provide design settings for commercial products.

Chapter 3 - Methodology

This section aims to provide an insight into the computational and experimental methodology that will be used in order to address this research objectives.

3.1 Mechanical Research Objective

The objective of this study is to investigate methods both computationally and experimentally that can be used to evaluate the mechanical performance of stents. The computational objectives of the research was to design simulations to assess longitudinal compression, flexibility and radial strength of various stent designs. These simulation provide computational models that evaluates mechanical performance, which can run numerous numerical solutions to identify stent structural performance for various designs.

The analysed stents were tested in the study for their mechanical performance in both compressive and bending stiffness, aiming to identify the stent structures for maximum bending, which can withstand compression. Future studies will involve improving radial strength of stents.

Compressive Stiffness: Maximise the compressive stiffness to withstand compressive forces.

Bending Stiffness: Minimise the bending stiffness to improve flexibility and deliverability.

Radial Stiffness: Maximise the radial stiffness to improve radial strength.

Compressive Stress: Maximum compressive stress to remain less than the yield stress with a maximum applied force.

Bending Stress: Maximum bending stress to remain less than the yield stress with a maximum applied force.

Radial Stress: Maximum radial stress to remain less than the yield stress with a maximum applied force.

The experimental studies objectives also focus on assessing mechanical performance. The compression experiment investigates the relationship between applied load and deformation of stent structures, which can be used to evaluate current commercial stents strength and for validating computational simulations. The deliverability experiments aims to determine the difficulty level of delivering commercial stents through complex pathways and investigating stent performance during delivery.

3.2 Computational Methodology

The methodology can be broken down into three main components, including: stent geometric model, design constraints and computational simulation.

3.2.1 Stent Geometric Model

The stent geometric model aims to create a computational model of a stent structure for numerical simulations in order to provide insightful results. The geometric model accuracy is important to the reliability of the results and the insight that can be achieve through varying various parameters. The parameters have been based on the design variables chosen in the study on hemodynamic in idealised coronary arteries: a multi-objective stent optimisation conducted by Heidi Wright and Jinbo Liu. This study provides an assessment of the stent geometries in that paper in terms of longitudinal strength. The stent geometries will be generated using Inventor and SolidWorks, varying the parameters suggested in Table 3.

3.2.2 Design constraints

The literature review evaluated various stent designs and parameters that can be considered. The constraint range is based on researched stent design parameters and values that are considered reasonable for varying the characteristics across. The study focuses on seven crucial design variables including: stent cross-sectional shape, stent dimension, strut angle, alignment type, cell height, connector type and number of connectors. The chosen design variables and constraint ranges are displayed in Table 3.

Table 3: Design Variables and Design Constraints

Design Variables	***Design Constraint Ranges***
Cross Sectional Shape (CS)	Rectangular or Circular
Strut Dimension 1 (SD1)	60-120 μm
Strut Dimension 2 (SD2)	60-120 μm
Intra-Strut Angle (SA)	25˚ - 50˚
Alignment Type (AT)	0˚ or 180˚
Cell Height (CH)	0.83 mm – 2 mm
Connector Types (CT)	1 = Straight 2 = Spline 3 = Semi-Circular
Number of Connectors (NC)	1 = One per ring 2 = Two per ring 3 = Alternating 1-2-1

An illustration of the design variables on a stent structure can been seen in the figure below. These parameters can be varied to create different geometric models.

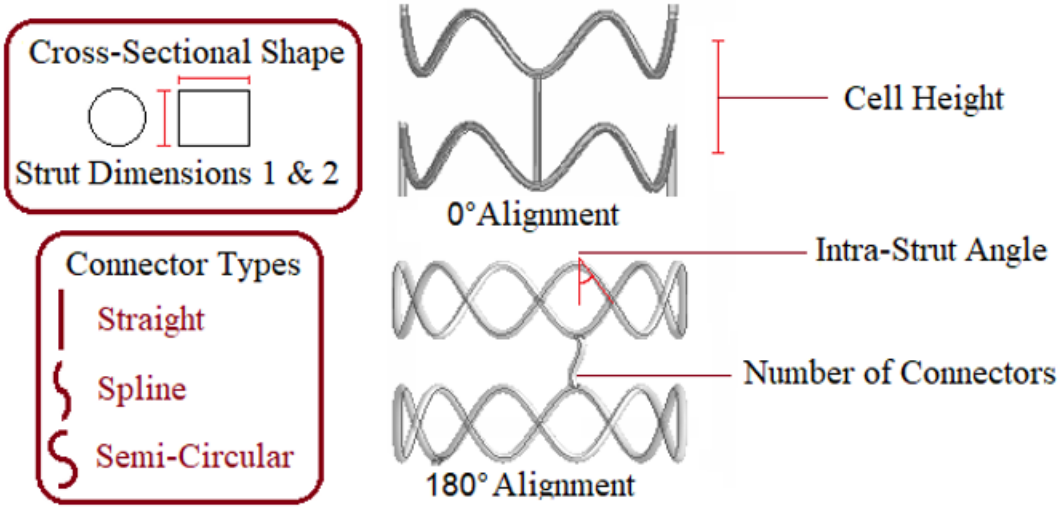

Figure 13: Design Variables

3.2.3 Computational Simulation

The Inventor geometries are imported into ANSYS Workbench 19.1 in order to perform numerical analysis on the structure in terms of mechanical characteristics. The computational simulations attempt to represent real world conditions in order to provide meaningful results. The simulations will use previous literature shown in section 2.4 of the literature review to aid in the assembly of the models. The composition of the simulation consists of four main components, including: mesh generation, mesh sensitivity, mechanical boundary conditions and analysis procedure.

3.2.3.1 Mesh Generation

The stent geometries will be meshed using a patch-conforming, unstructured tetrahedral mesh with variable mesh spacing. In addition grid sizing will be utilised to provide a layered thickness for the wall of the stent to allow for an accurate analysis of the changing structure. Figure 14 displays the geometries and mesh for the validation simulations for both the bending and compression simulations. For the bending simulation a coarse mesh was applied to the supports a no analyse was being conducted on the cylindrical support performance. This allows for a reduction in mesh density, hence lower computational time

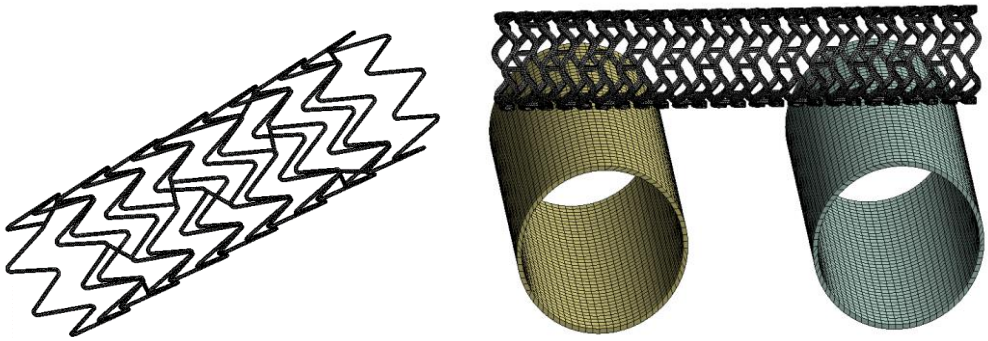

Figure 14: LHS meshing for compression validation simulation, RHS meshing for bending flexibility validation simulation

3.2.3.2 Mesh Sensitivity Study

The simulations were solved using ANSYS 19.1 is a commercial software, which uses numerical procedures to solve complex problems. For verification a mesh convergence study was conducted. This was done in order to determine the level of refinement of the mesh required to achieve appropriate deflection in the compression and bending simulations, without requiring further refinement.

The convergence study for the compression simulation was conducted across fourteen characteristic length for both the rectangular and circular cross-sections. The system solved for a finite element setup of stent 1 for the circular cross-section and stent 19 for the rectangular. Below displays the mesh convergence study for the static structural situation.

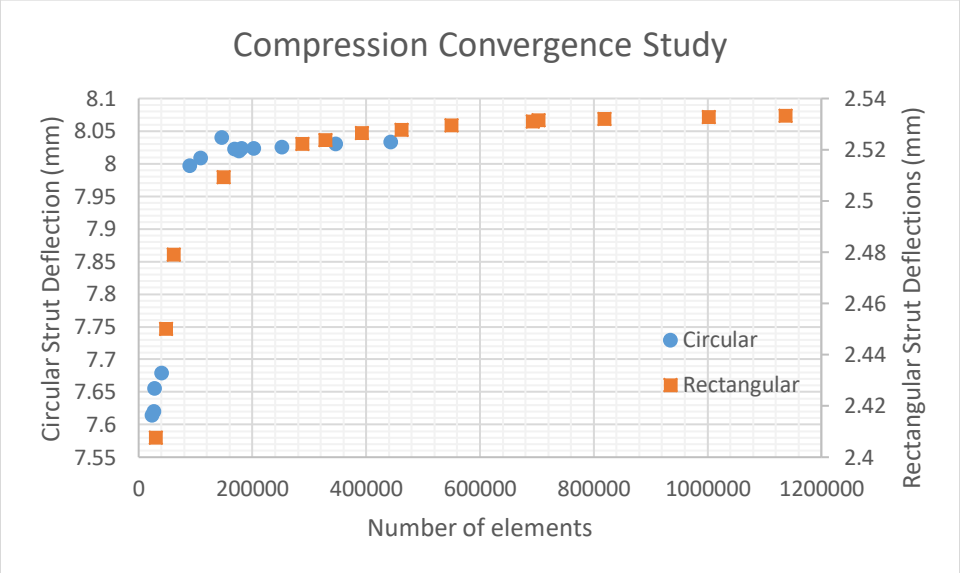

Figure 15: Compression Convergence Study

To display the independence of the solution compared to the mesh density, the deflection caused by compression of the stent structure were monitored for each characteristic length. The results from the mesh convergence study demonstrated that the solution became independent when the characteristic length created a mesh density of at least 300,000 elements for both cross-section dimensions. Therefore, a mesh density of at least three hundred thousand can be selected for further calculations to reach faster computational time, while achieving equivalent data.

The convergence study for the bending simulation was conducted across fourteen characteristic length for both the rectangular and circular cross-sections. The system solved for the same stents as the compression independence study. Below displays the mesh convergence study for the bending situation.

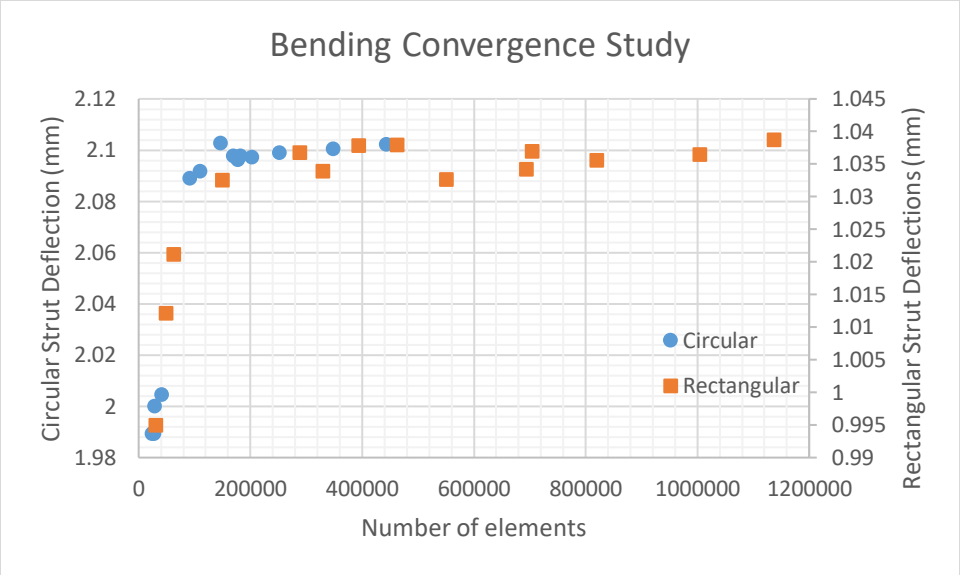

Figure 16: Bending convergence study

The results from the mesh convergence study demonstrated that the solution became independent when the characteristic length created a mesh density of at least 200,000 elements for both cross-section dimensions. Therefore, a mesh density of at least two hundred thousand can be selected for further calculations to reach faster computational time, while achieving equivalent data. This mesh sensitivity study allowed for accurate data collection while reducing computational time.

3.2.3.3 Boundary Conditions

Boundary condition are set in place to constrain the system and allow for analysis to be done to investigate certain aspects. The compression system will only be affected by a compression force and aims to simulate a bench test scenario. For the static structural analysis the base of the stent will be fixed and constrained in all principle directions, while having a constant load being applied to the opposite end. The stent aims to distribute the force across the stent structure aiming to reduce the stress effecting the rings and struts. The boundary conditions are displayed in Figure 17.

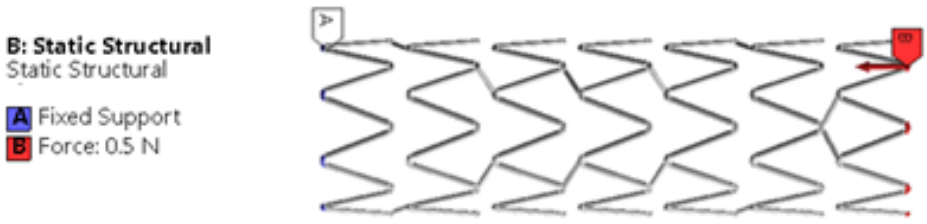

Figure 17: Compression Study Boundary Conditions

For the bending simulation two cylindrical structural supports will be fixed for the duration of the structural analysis. An applied force will be inflicted to the centre ring causing the cylindrical supports to provide a reaction force and in turn causing the stent to bend. The boundary conditions are displayed in Figure 18.

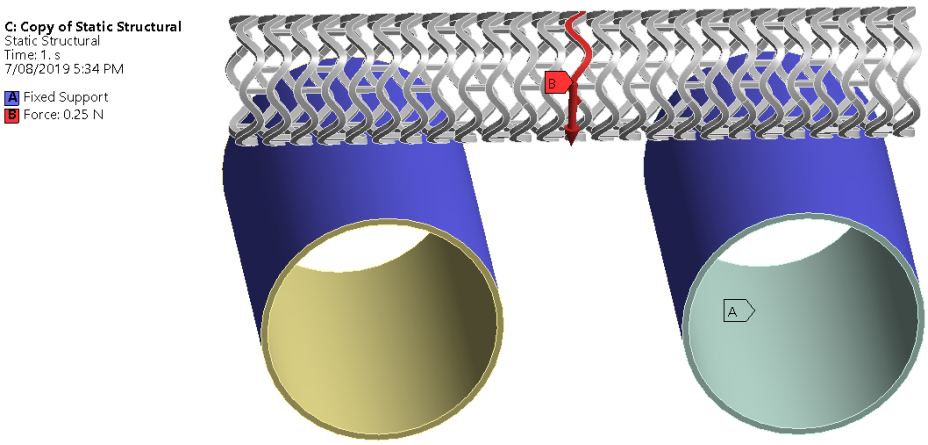

Figure 18: Bending Simulation Boundary Conditions

A third mechanical study was constructed due to the COVID-19 outbreak halting project progress in other aspects. The mechanical study investigated the radial strength of stents. The study focused on the rings of the stent and applied a displacement boundary condition around the middle of the ring. The displacement constricted movement in the z and y axis of a cylindrical coordinate system and allowed for free movement in the x direction. A pressure was then applied to the outside surface of the ring, representing the pressure provide by the vessel wall. These boundary conditions enables the stent ring to compress radially by increasing the applied pressure.

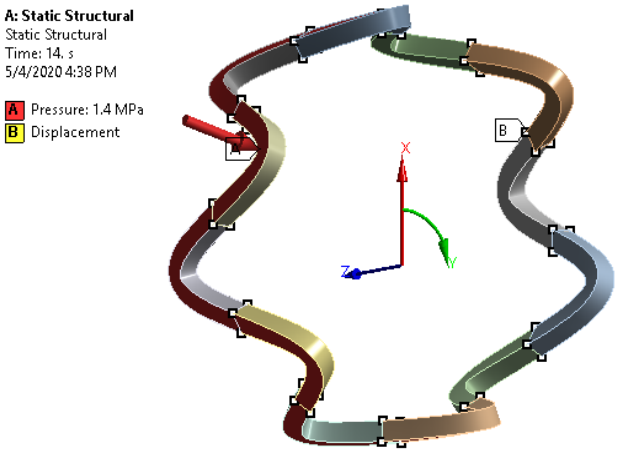

Figure 19: Radial Test Boundary Conditions

3.2.3.4 Analysis Procedure

The simulation will be setup with the boundary conditions shown in section 3.2.3.3 to allow for an accurate examination of mechanical characteristics. For preliminary work a validation study will be performed on the simulations to match previous literature in order to prove the reliability and validity to the simulation. Once the simulations have been validated, analysis can be done on the data collected from the numerical solution. The results can then be derived from the solution solved by ANSYS.

3.2.3.4.1 Compression Simulation

The compression simulation will use the maximum deformation and the Hooke's Law principle to determine the compressive stiffness of the stents.

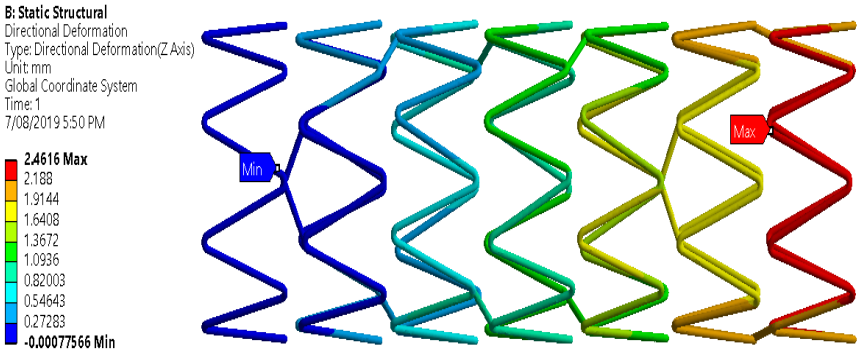

Figure 20: Results for compression validation simulation

The compressive stiffness of the stents are calculated using Hooke's Law, which demonstrates that materials have a linear region where the stress verse stain are proportional. Within a certain limit of the elastic region of a material, the force required to compress/extend an object is directly proportional to the compressed/extended length. The commonly known Hooke's Law can be written as:[35]

$$\boldsymbol{F = -kx}$$

The proportional constant is k, which is the spring constant that measures the stiffness of the object. The force the object exerts to counter the applied force is known as the restoring force, it acts to restore the object to its equilibrium length. [35] Hooke's law is remarkably general and can be used for any object that can be distorted by a force, where the restoring force is proportional to the displacement from equilibrium. However, when the distortion becomes too large the linear elastic limit is reached providing a non-linear trend. Until the elastic limit is reached, Young's modulus is the property of the material which is used to predict the elongation and compression stiffness through Hooke's Law. [36]

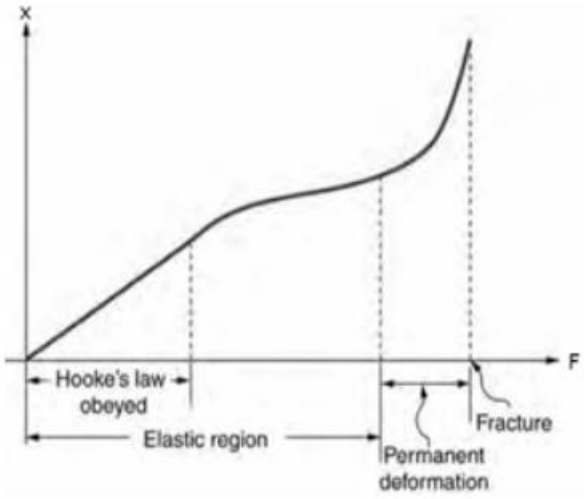

Figure 21: Hooke's Law limit in elastic region

3.2.3.4.2 Bending Simulation

The bending simulation will use the maximum deformation, which occurs in the centre of the stent structure to determine the bending stiffness of the stents. The stiffness will be calculated using the equations based on beam theory.

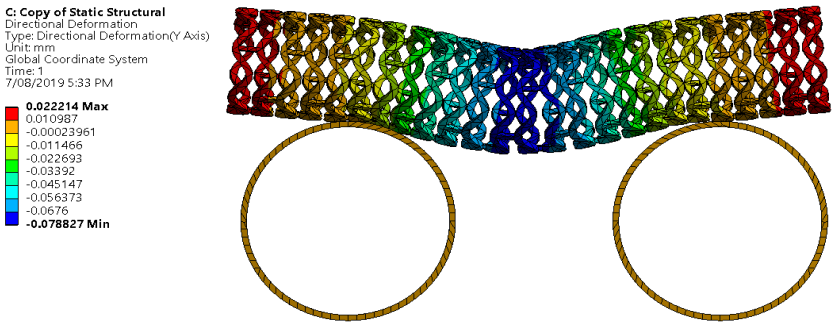

Figure 22: Results for bending flexibility validation simulation

The bending flexibility of a stent can be represented as a stiffness value. The larger the bending the stiffness the greater the force required to bend the stent, hence a lower flexibility. The bending stiffness of a stent can be calculated using the following equation:[32]

$$\boldsymbol{Bending\ Stiffness}: EI = \frac{Fl^3}{48f}$$

The relationship between the bending deflection and the point force is based on the beam theory. The bending theory is based on the Young's modulus of a material. If an applied load is placed on a three point bending system a linear relationship will remain within the elastic limit of the material[37].

3.2.3.4.3 Radial Simulation

The radial strength simulations can use the average total deformation to determine the radial strength of the rings for the material in the elastic region. The stiffness can be calculated based on the deformation rate of the structure due to an applied load.

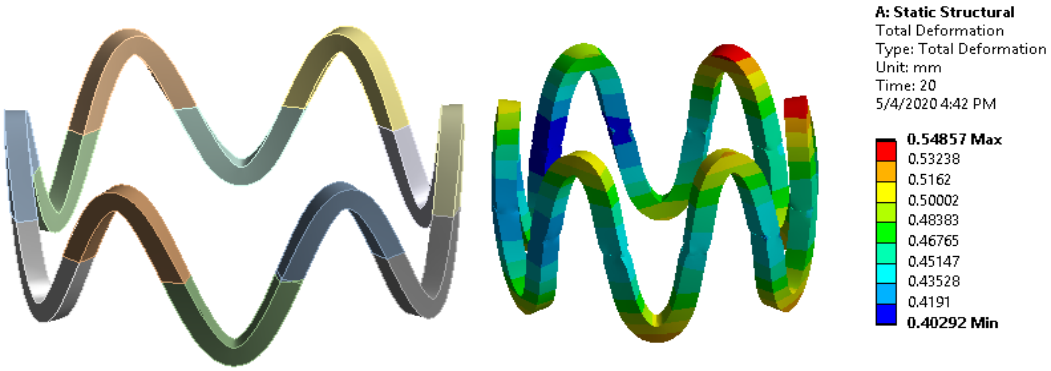

Figure 23: Before and after versions of radially compressed stent ring

This strength can be analysed by evaluating the change in diameter in relation to the applied radial force. The force is determined by using the pressure and surface area of the outer area of the stent. The radial stiffness of a stent can be calculated using the following equation:

$$\boldsymbol{Radial\ Stiffness} = \frac{F}{D}$$

The relationship between the change in diameter deflection and the applied force can be used to determine the radial stiffness. If an applied load is placed on the outside surface of the system a linear relationship will remain within the elastic limit of the material[37].

3.2.3.4.4 Stress Analysis

The stents will also be analysed for the maximum Von Mises Equivalent stress to assess the stress on the stent and when it surpasses yield stress causing permeant deformation. The elastic modulus is used as a numerical constant and describes the elastic properties of a solid, which is experiencing a load causing elongation or compression lengthwise. This modulus helps describe how a material will perform based on change in length under the given conditions. The modulus is basically the stress strain relationship of a material, as displayed in the figure below.[38]

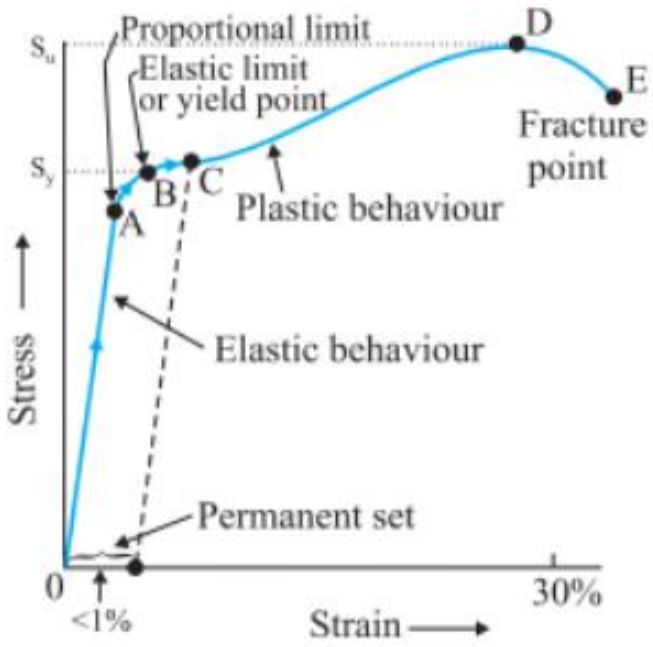

Figure 24: Young's Modulus chart [38]

There are various stages involved in the material behaviour. A material under loading will demonstrate elastic behaviour which is a linear relationship until it hits the proportional limit. Once it passed the proportional limit the material experiences non-linear elastic behaviour. Once the material passes the elastic region, the material demonstrates plastic behaviour until finally fracturing. If you distort the object past the elastic region the object is likely to become permanently deformed, fracture or have weak structural integrity.

During the mechanical analysis the stent behaviour is monitored during the elastic regions as the plastic region can have major impacts to the structural strength. The structures will be examined for maximum compressive, radial and bending stresses to avoid permeant deformation and determine when stresses past the yield point.

3.3 Material Performance Comparison

The composite materials were analysed for each of the structures, but for simplicity comparison will be done on three different stent geometries across four different material options. Various materials will be analysed as some materials are able to provide a high strength to weight ratio. Composite materials are made of a combination of two or more materials to create a unique material with diverse properties. Advantages of composite materials include:[39]

- High strength to weight ratio
- Material is more malleable
- Excellent fatigue endurance and residual fatigue strength
- Excellent chemical resistance

Research was performed to examine the most commonly used materials for stents to provide an analysis that was commercially relevant. Four materials were included in the study, including: stainless steel, platinum chromium, cobalt chromium and magnesium alloy. The material properties used have been summarised in Table 4.

Table 4: Material Properties

Material Properties	***Stainless Steel [40]***	***Platinum Chromium [31]***	***Cobalt Chromium [41]***	***Magnesium Alloy [32]***
Young's modulus [MPa]	200 000	203 000	210 000	45 000
Poisson ratio	0.3	0.285	0.29	0.35
Density [Kg/m^3]	7850	7850	10000	1800
Tensile strength [MPa]	460	834	1500	460
Yield point [MPa]	250	480	1000	188

3.4 Deliverability Experimental Protocol

3.4.1 Aim:

The aim of the experiment is to determine the deliverability of various commercial stents by performing bench testing.

3.4.2 Objectives:

The objective of the experiment is to determine the deliverability of various commercial stent through a complex system. Then evaluate the bending curvature required to cause stents to fail during implantation and analyse the structural response to different degrees of bending.

3.4.3 Apparatus:

- Commercial Stents with delivery equipment (Eg: guide wire, catheter, etc)
- Plastic grid with holes
- Zip ties
- 3mm diameter tube
- Camera

3.4.4 Experimental Setup:

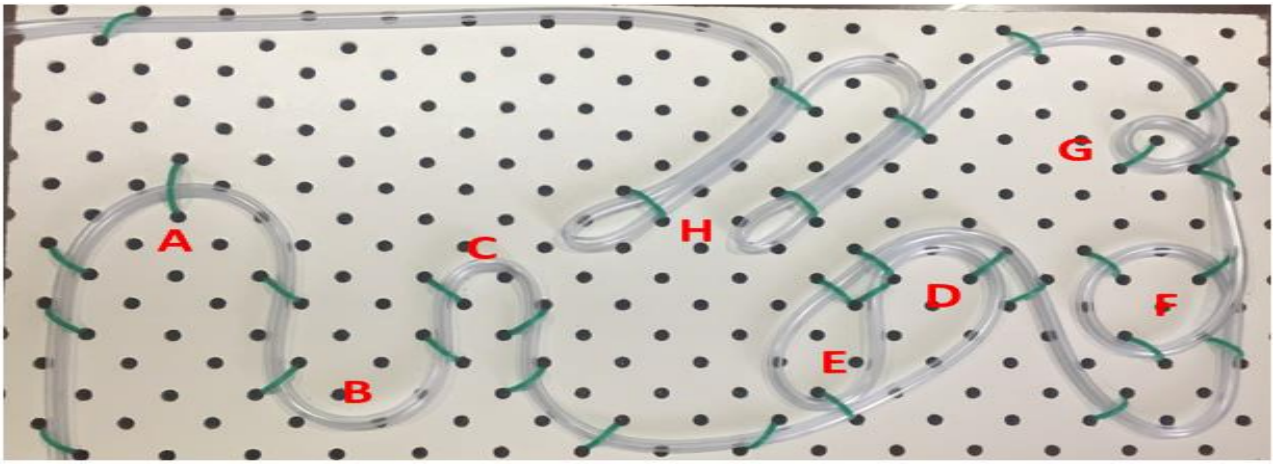

Figure 25: Experimental setup

3.4.5 Method:

1. Setup the system with the tube moving in the desired pathway.
2. Feed the stent delivery mechanism into the system similar to the method used during procedures.
3. Use the camera to record the stent structure reaction at different bending sites.
4. Record findings on feedback questionnaire.

3.3.6 Analysis:

Analysis will be performed by recording the stent structure reaction at each labelled bending junction. The curvature at each junction can be seen in Appendix A. Following the experiment the surgeon will complete a questionnaire based on evaluating the experience and improving the design of the experiment. The questionnaire can be found in Appendix B.

3.5 Compression Experimental Protocol

3.5.1 Aim:

The aim of the experiment is to determine the compressive stiffness of various commercial stents by performing bench testing.

3.5.2 Objectives:

The objective of the experiment is to investigate the relationship between force and compression length of various commercial stents. Examine at both high and low loading cases. Then determine the compressive stiffness of current commercially available stents and perform analyse on the structural response at a maximum loading case. (0.5N based on Ormiston's Paper)

3.5.3 Materials:

- Commercial Stents
- Stent connection pins
- DMA machine

3.5.4 Experimental Setup:

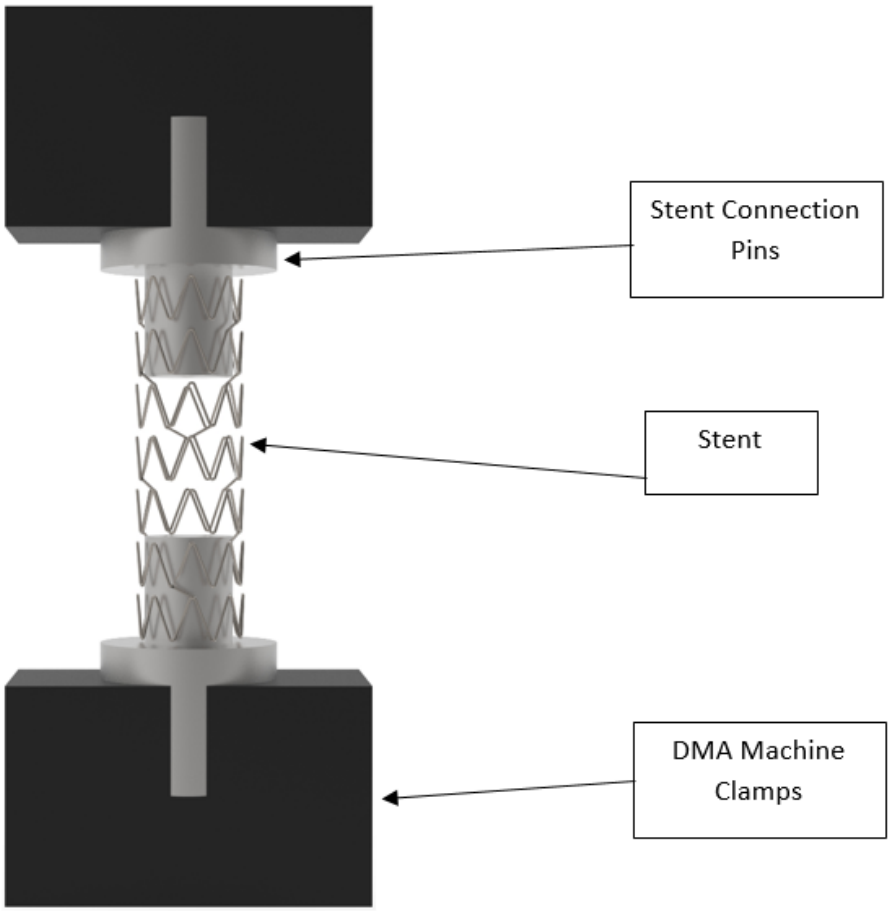

Figure 26: Compression Experiment Setup

3.5.5 Method:

1. Clamp both stent connection pins into the DMA machine.
2. Place the stent on the base connection pin.
3. Align the cylindrical section of the top connection pin with the inside diameter of the stent.
4. Slowly move the top connection pin down until the cylinder of the top connection pin is inside the stent.
5. Continue to move the top connector down until the base of the top connection pin is tangent to the top hoop of the stent.
6. Then move the top pin connector down in increment of 0.1mm recording the applied force or vice versa, apply a force of 0.02N and record the compression displacement.

3.5.6 Analysis:

Analysis will be performed by recording the compression displacement and applied force at different increments. Based on these results a calculation on the compressive stiffness using displacement and force values can be performed. Images will be taken of the stents at different increment and at maximum compression for comparison.

Chapter 4 – Results

4.1 Validation of Simulations

The validation study aimed at creating computational simulations that match previous literature. The data was collected using the methodology discussed in section 3. The experimental data was collected from the paper Stent longitudinal integrity bench insights into a clinical problem by Ormiston and used to evaluate the accuracy to the numerical solutions. These results focused on the compression strength of the commercially available Omega stent. Figure 27 displays the correlation between the experimental data from literature and the computational data retrieved from the simulations.

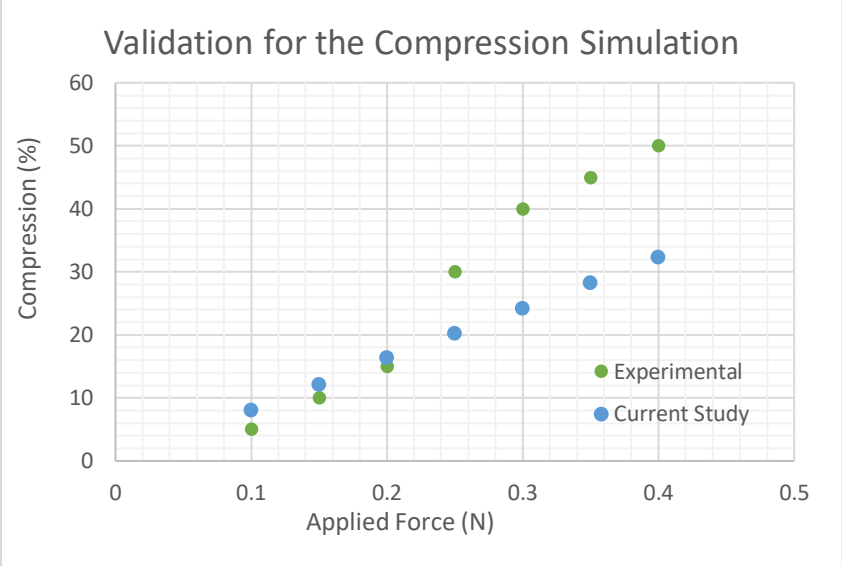

Figure 27: Compression Strength of Omega Stent

The data from Figure 27 show similar trends between the results, displaying a linear relationship between the deflection and the applied load. The results agreed well for experimentally derived compression behaviour, especially for smaller forces applied (< 0.2 N with < ±0.25mm difference). Stents appeared to deform 15-20% (1-1.8mm) less computationally compared to the experimental data for larger loads (> 0.2 N). This difference may be due to inconsistency in measuring the strong stent displacement once deformed. The discrepancies of the experimental data could be due to the level of accuracy of the measuring equipment, impurities in material and quality issues of the stent for the results retrieved from the literature.

The simulation focus on optimal stent designs with a stronger compressive stiffness to reduce the amount of deflection to prevent damage due to recoil when the stent springs back. Also at higher deflections the stent is also more prone to move into plastic region of deformation causing permanent structural changes and potentially fracturing. In general, the simulation was considered valid for the elastic region of mechanical performance due to good correlation between results.

Computational simulation has been performed on establishing the bending flexibility of coronary stents. A paper on Improvement of Mechanical Performance of Bioresorbable Magnesium Alloy Coronary Artery Stents through Stent Pattern Redesign performed by Wang et al. was used to validate the numerical simulation. These results used a three point bending method to establish the deflection in the middle of a stent due to an applied force. Figure 28 displays the correlation between the experimental data from literature and the computational data retrieved from the simulations.

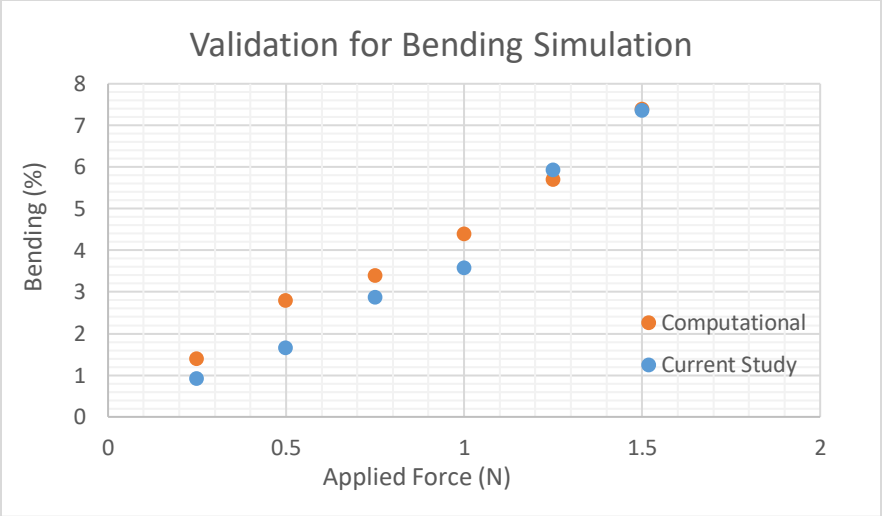

Figure 28: Validation on Bending Flexibility

The results displayed in Figure 28 show a good correlation between the experimental and computational results. Both have similar trends indicating good accuracy for the numerical simulation. The bending simulation agreed well with other computational data, with less than a ±0.05mm (1.1%) difference. This indicated the simulation demonstrated good accuracy for determining deflection during a three point loading scenario.

Due to the COVID-19 situation a third simulation focusing on the radial strength of stents was conducted. A paper on Design Methodology of a Balloon Expandable Polymeric Stent by Avinash Kumar et al. was used to validate the numerical simulation. These results used the ring of the stents and examined the radial strength by applying a pressure on the outside surface of the ring[34]. Figure 29 displays the correlation between the computational data from literature and the computational data retrieved from our current study.

The data from Figure 29 shows similar trends between the results during the elastic phase, displaying a linear relationship between the deflection and the applied load. The results agreed well for compression behaviour when smaller forces were applied (< 1.2 N with < ±0.06mm difference). Stents appeared to deform differently computationally in the current study compared to the literature simulated data for larger loads (> 1.2 N). The discrepancies could be due to the way the material reacts due to larger stresses. The material behaviour in the literature matches Figure 24 in section 3.2.3.4.4, with the convergence in the literature values demonstrating plastic behaviour of the materials. This indicates the simulation accurately represents the elastic behaviour of stents, but will need improvements if the study requires evaluation of the structural performance during plastic behaviour of the material.

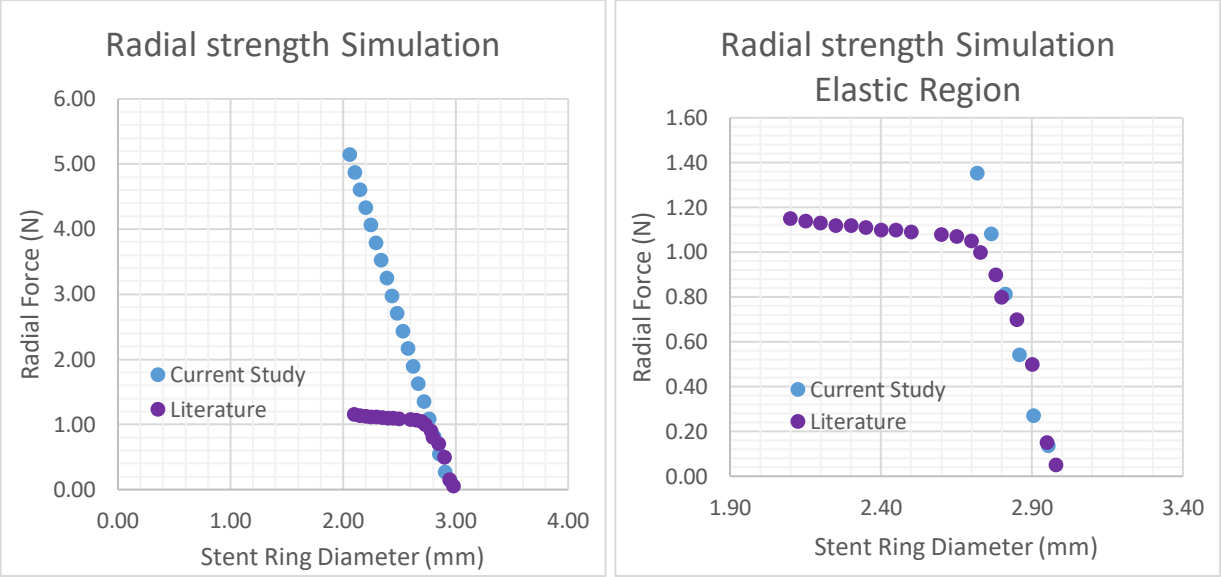

Figure 29: RHS Radial Strength Simulation comparison, LHS Simulation results zoomed in on the Elastic region of material

4.2 Mechanical Integrity Assessment

This study used simulated results from Heidi Wright and Jinbo Liu study on optimising stent structures in terms of haemodynamic flow to assess the non-dominant solutions for mechanical integrity. There were a total of 19 non-dominant solutions derived from the study containing both cylindrical and rectangular cross-sections. Stent 7 was unable to be generated thus only 18 (of 19) were analysed. The variable allocation and respective objective outcomes for each stent structure can be seen in Table 5.

Table 5: Mechanical analysis of hemodynamically optimised stents

Name	CS	SD1 (µm)	SD2 (µm)	SA (°)	AT (°)	CH (mm)	CT	NC	Comp Stiffness (N/mm)	Bending stiffness (N/mm^2)	Bending Stress (MPa)	Comp Stress (MPa)
S1	**Circular**	60	NaN	28.799	0	0.917	2	1	0.001	0.072	97	4969
S2	**Circular**	60	NaN	25.652	0	1.274	2	1	0.002	0.075	270	11937
S3	**Circular**	60	NaN	31.844	0	1.176	2	1	0.002	0.082	144	4990
S4	**Circular**	67	NaN	29.583	0	0.889	1	1	0.002	0.102	100	3727
S5	**Circular**	65	NaN	42.917	0	1.084	1	2	0.036	0.810	271	865
S6	**Circular**	71	NaN	31.250	0	1.045	2	1	0.003	0.101	104	3036
S7	**Circular**	63.7511	NaN	32.995	0	1.251	1	1				
S8	**Circular**	73	NaN	38.750	0	1.669	3	1	0.005	0.158	128	2805
S9	**Circular**	60	NaN	43.936	0	1.373	1	2	0.034	0.430	268	958
S10	**Circular**	65.2947	NaN	43.358	0	1.305	1	2	0.048	0.660	472	1584
S11	**Circular**	95	NaN	45.417	180	1.942	1	1	0.019	0.645	173	1215

S12	**Rectangular**	63	81	43.750	180	1.786	3	1	0.007	0.334	213	2510
S13	**Rectangular**	61	109	27.917	0	1.630	2	3	0.014	0.474	202	2201
S14	**Rectangular**	75	101	41.250	0	1.708	2	1	0.010	0.442	387	1544
S15	**Rectangular**	93	67	32.917	180	1.981	2	1	0.014	0.351	139	1850
S16	**Rectangular**	109	89	42.083	180	1.591	3	2	0.473	5.256	470	192
S17	**Rectangular**	103	75	32.083	180	1.474	1	1	0.018	1.865	827	1013
S18	**Rectangular**	89	83	37.917	0	1.006	1	3	0.009	0.658	226	1426
S19	**Rectangular**	115	95	37.083	0	1.201	3	3	0.040	1.465	269	790

4.3 Initial Sample Performance

The results from the simulations have been displayed in the graphs below. Figure 30 shows the spread of the results and demonstrates that one stent (S16) has a much stronger compressive stiffness and bending stiffness. In order to fully analyse the results a graph was created without stent 16 to evaluate the performance of the other stents.

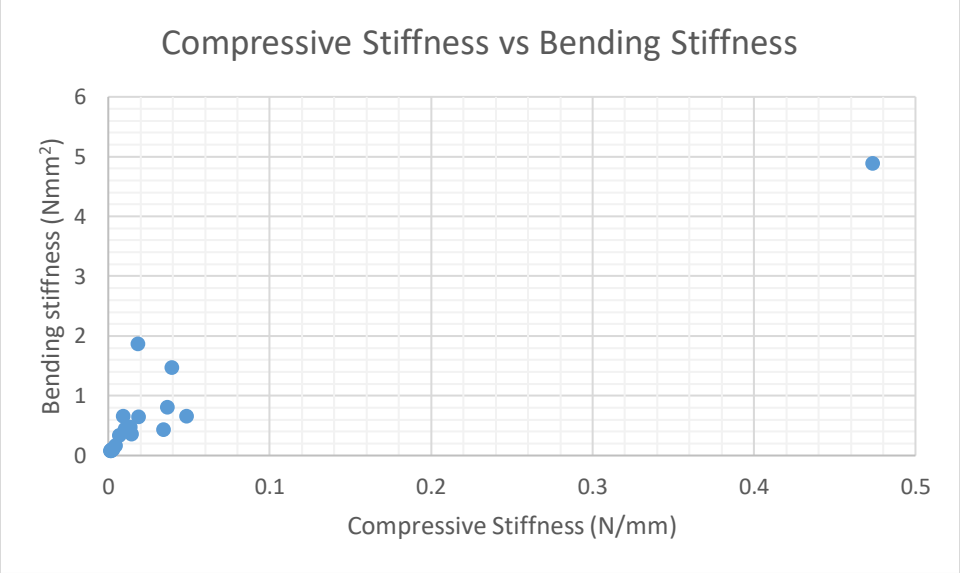

Figure 30: Compressive stiffness vs bending stiffness (with stent 16)

Figure 31 below visually demonstrates the trade-off of the objectives, where an increase in compressive stiffness increases the bending stiffness. The optimal solution has a high compressive stiffness and a low bending stiffness, hence the low right corner of the graph. Majority of the results demonstrate a low compressive and bending stiffness, indicating they have a strong deliverability performance but will compress more easily, which could cause damage during recoil back to original length.

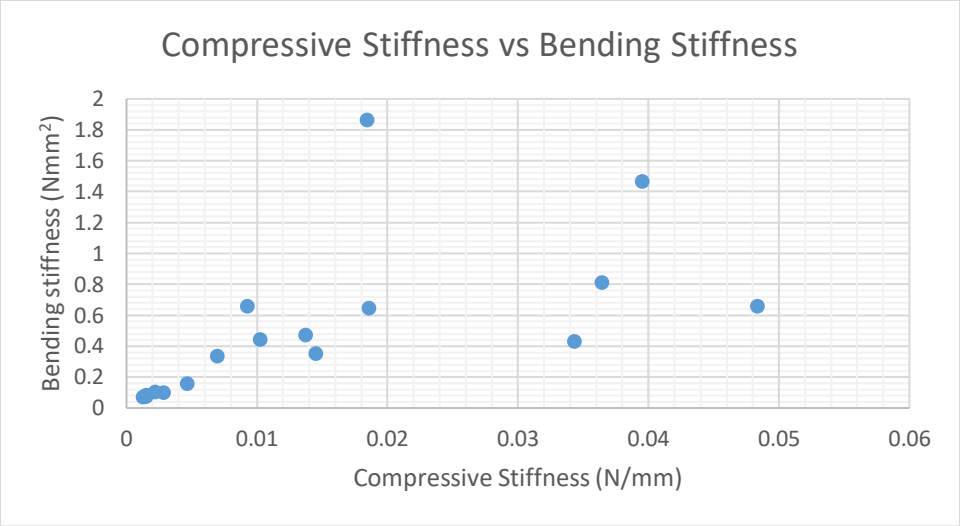

Figure 31: Compressive stiffness vs bending stiffness (without stent 16)

4.4 Material Comparison Simulations

A material comparison was performed by analysing four different types of material for three different types of stent structures. Each stent structure was chosen specifically to represent significantly relevant geometries, while having considerable differences. The Omega stent provided results for a commercially used cylindrical stent. The bending stent was used from the validation study and provided results for a larger strut diameter (0.15mm) with an increased volume of rings and straight connecters, having three connector per ring. Stent 16 was the best performing stent for the structures assessed for mechanical performances that were optimised for haemodynamic flow.

The results in Table 6 display similar results for Stainless Steel, Platinum Chromium and Cobalt Chromium. The results found that cobalt chromium had the best compressive strength and that magnesium alloy had the most flexible properties. Each stent showed the same trend in performance between each material indicating the results reliably demonstrate the performance of material for different stents.

Table 6: Material comparison for stents

	Omega Stent		**Bending Stent**		**Stent 16**	
Material	**Compressive stiffness (N/mm)**	**Bending stiffness (N/mm^2)**	**Compressive stiffness (N/mm)**	**Bending stiffness (N/mm^2)**	**Compressive stiffness (N/mm)**	**Bending stiffness (N/mm^2)**
Stainless Steel	0.12	1.49	10.25	336.72	0.47	5.17
Platinum Chromium	0.12	1.51	10.38	341.19	0.47	5.26
Cobalt Chromium	0.13	1.56	10.74	353.14	0.49	5.43
Magnesium Alloy	0.03	0.33	2.26	58.64	0.10	1.16

4.5 Research Opportunity and Performance Evidence (ROPE)

This section of the report aims to establish the changes that have been implemented due to the COVID-19 circumstances and explain the affect this has had on the outcome of the report. The COVID-19 situation mainly impacted the progress of experimental work as the hospital became very busy making it harder to work with the surgeons and laboratories were shut down for an extend period of time. The impact mainly affected the deliverability experiment and compression experiment. These experiments were researched, protocols were designed and manufacturing streams were identified and contacted. Although, due to the COVID situation they were heavily delayed and were unable to progress to completion.

The deliverability experiment was heavily delayed due to the COVID-19 situation with only initial surgeon feedback being provided on the testing system and analysis protocol. An experimental protocol and setup of the system was constructed within the first half of the semester. I was only able to meet with the surgeons in week 11 to discuss the design of the system, gain feedback for adjustments and test the system with an appropriate delivery system for improvement purposes. Most of what was achieved was feedback for improvements which will be discussed in section 6. If there wasn't a COVID situation, an improved experimental setup could have been designed and tested properly following the experimental protocol. Unfortunately, the experiment could not progress past the feedback stage to a position providing relevant results for discussion.

The compression experiment was even more heavily delayed with only an experimental protocol being constructed and partially reviewed. The protocol was analysed by a student who uses the DMA machine for research. The student believed improvements to the pin connectors was necessary, but due to being quarantined in another country was not able to discuss how improvements could be made to the design. Additionally, due to the reduced amount of laboratory work throughout UNSW, training and working with the DMA machine was not possible.

Although the experimental work was considerably reduced due to the COVID situation, more work was performed on computational simulations to continue progress with mechanical analysis. A simulation was designed for examining the radial strength of stents and a material comparison was performed on commonly used stent structures. While the experiments were not performed to their full extent, enough planning and information has been recorded for someone in the future to continue the experimental work.

Chapter 5 – Discussion

The relationship between the mechanical objectives is a balancing problem between the characteristics as advancements of one aspect can have a deteriorating effect on another aspect. This investigation ambitiously endeavoured to consider seven important geometric variables for two objective outcomes and two constraints. The assessment of the mechanical integrity of the hemodynamically optimised stents provided great insight into the structural performance. Figure 32 provides a performance comparison between the circular and rectangular cross-sectional shapes. The rectangular cross-section demonstrated a higher bending stiffness and a comparable compressive stiffness. This indicates that the rectangular shape displays positive results for mechanical performance, which is important to consider since circular cross-sections are highly dominant in the commercial market for stents.

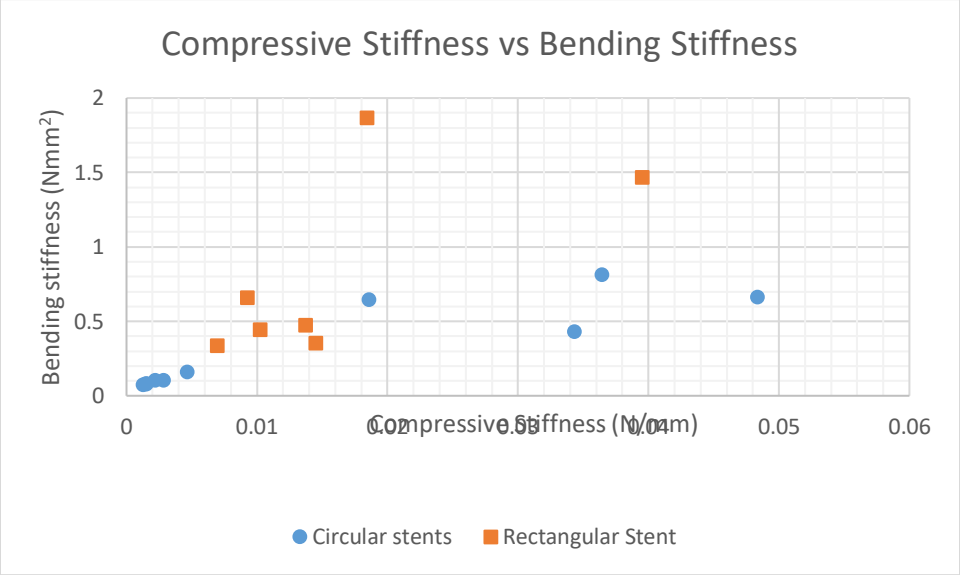

Figure 32: Circular and rectangular cross-section comparison

The most significant aspect affecting the longitudinal mechanical performance of stent is the connector type and configuration. Figure 33 demonstrates the effect of the connector type and number of connectors had on the performance of the structure. Straight connectors had greater stiffness properties, while the spline and semi-circular connectors demonstrated lower stiffness values. This generally makes sense since the spline and semi-circular connectors can act more like springs storing the applied load compared to a straight connector which is more rigid. The number of connectors graph demonstrates that stents with one connector between the rings have considerably lower compressive and bending stiffness. Having two connectors between each ring provided a much greater compressive stiffness without severely increasing the bending stiffness. Based on the data collected and analysing the stress results in Table 5 it was evident that single connectors between the rings demonstrate a considerably weaker mechanical performance under loading and would contain a much higher fracture rate. Therefore, it was determined in order to improve mechanical performance stents require at least two connectors. This was then further supported through research and discussions with surgeons establishing that one connector stents are very uncommon.

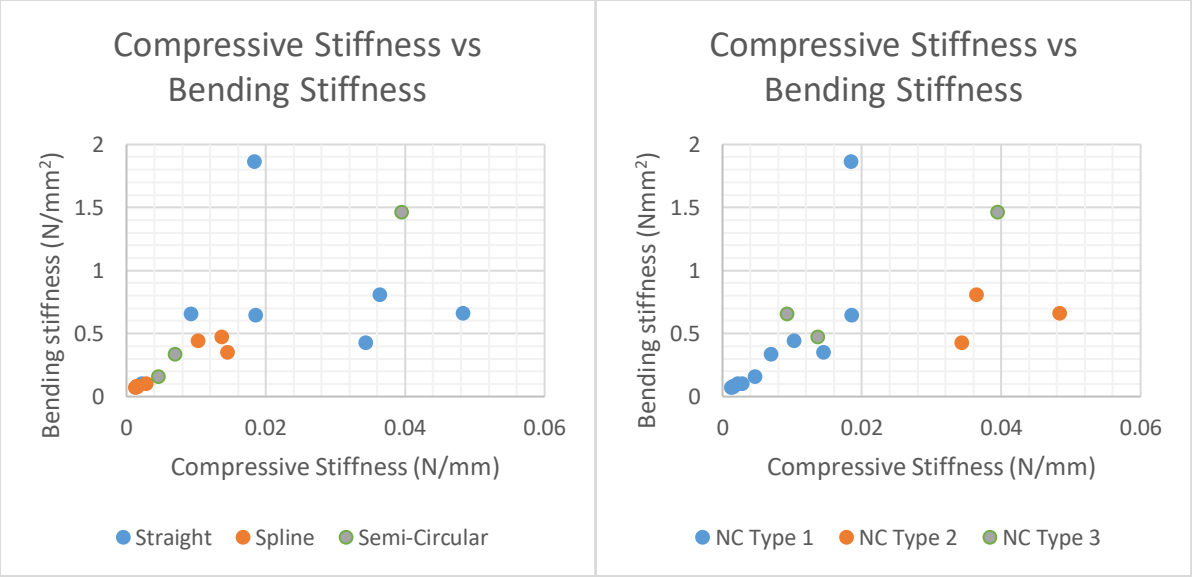

Figure 33: Mechanical performance of connectors

Table 7 provides a comparison between the simulated results from the current study with the mechanical performance of commercial stents. For a more detailed table on the commercial stents mechanical performance see Appendix C. When compared to commercial stents only stent 16 seemed to fit within the normal range. Stent 16 provided a very strong compressive stiffness of 0.47 N/mm and a mid to high ranged bending stiffness of 5.26N/mm^2. This indicates that the hemodynamically optimised stent 16 would perform effectively under mechanical loading. Majority of the stents showed a considerably weaker compressive stiffness (<0.05 N/mm) and bending stiffness (0.074-1.86 N/mm^2). This indicates that the stent structures can afford to become more stiff and rigid to provide greater compressive strength, which in turn will increase the bending stiffness, but the results show the structures can afford to be less flexible, and still perform effectively. This comparison made it evident that the structures need to become stiffer as being too flexible could prevent the stent from effectively reducing stenosis and being weak compressively will increase damage caused by stent recoil whenever the stent is compressed. Overall, this comparison demonstrated that stents optimised for hemodynamic flow will fail mechanically when implanted, unless the structure is examined for different stress and loading conditions.

Table 7: Mechanical performance comparison with commercial stents

Type	**Commercial Compression Stents**	**Commercial Bending Stents**	**S16**	**Other Stents**
Thickness (µm)	100-81	100-81	109x89 (rectangular)	120-60
Connector Number	2 or 3	2 or 3	2	1 or 2
Compressive stiffness (N/mm)	0.16-0.53		0.47	<0.05
Bending stiffness (N/mm^2)		0.62-8.65	5.26	0.074-1.86

In order to further analyse the mechanical performance of the stents a material comparison study was conducted using commonly used stent materials. Figure 34 visually shows the differences between each materials performance for the Omega stent. The discrepancies between the materials were consistent for the other two stent geometries. The results found that cobalt chromium had the best compressive strength with 0.128 N/mm and that magnesium alloy had the most flexible properties with a stiffness of 0.333 N/mm^2. Overall it was found that the best materials to use would be platinum chromium, cobalt chromium or stainless steel as magnesium is considered to be too weak of a material and may fail more often. In general this project has collected useful data on material performance which can be used to improve stent designs.

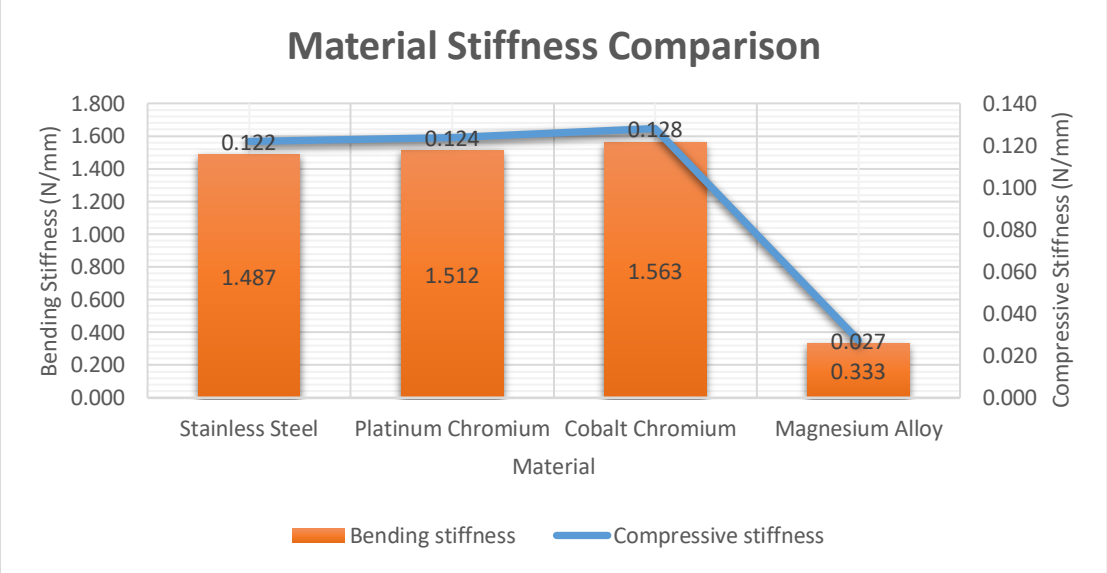

Figure 34: Material stiffness comparison

In additions to the computational simulations experimental work was conducted to determine mechanical performance in a practical application. Due to the COVID situation limited experimental work could be performed, but some preliminary feedback was provided from surgeons on the deliverability experiment. Figure 35 displays the surgeons implanting the delivery system into the constructed rig.

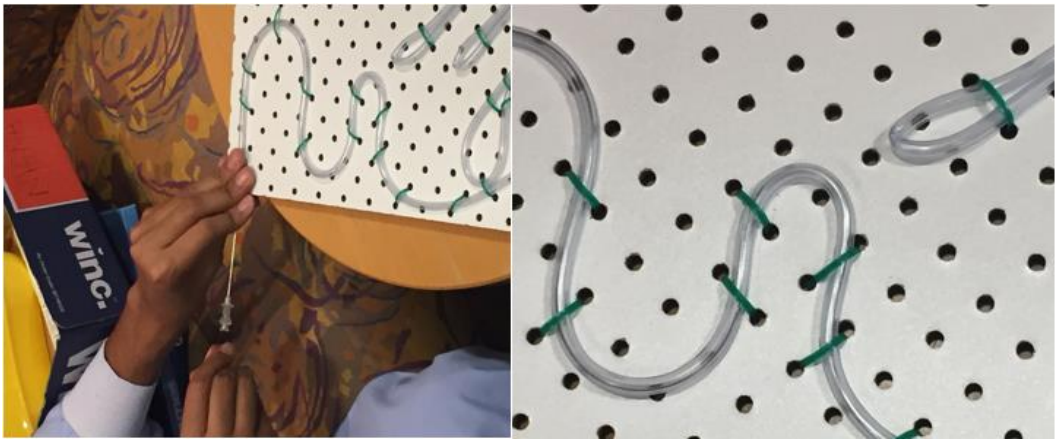

Figure 35: Deliverability experimental work

During the discussion with the surgeons improvements were discussed for the design, which could be implemented before running tests on a larger sample of surgeons. The effectiveness of delivering stents at each phase was evaluated using the questionnaire seen in appendix B. The improvements to be implemented to the delivery experimental system include:

- Shortening the sections from a continuous pathway to a new version with segments containing different curved structures. An example can be seen in Figure 36 with the system separated into different sections increasing in difficulty. The main reasons for shortening the system is because the delivery system is around 15 cm in length so it cannot handle a long pathway and the resistance due to friction significantly increases as the delivery system moves a long distance through the pathway.
- Changing the inside diameter of the tube at specific sections to act as lesions. This could be incorporated by 3D printing tube sections with lesions to understanding the major impacts of lesions on delivery outcomes.
- Potential 3D print a setup as seen in Figure 36 which has different pathways with different levels of complexity. In addition, constructing a staging area for the constructed setup to fix into so that the system more accurately represents the path of delivery before encountering the vessels near the heart.

The feedback from the surgeons provided useful information which will be incorporated for the new delivery system setup. The surgeons found that manipulation of the guidewire and catheter was fairly realistic in the model compared to live patient. The major differences being the vessel wall material felt different, the technique for controlling the wire was slight different as the surgeon knew the exact pathway and the clinicians used a more forceful technique to push the stent through compared to real life. The surgeons believe that their catheter and guidewire handling skills could improve by training on this model because even though the delivery feels different the principals involved for implantation are the same and the system would be useful for understand the mechanics of the procedure. The surgeons also believe that the model pathway accurately displays obstacles that would occur on the delivery of a stent through a vessel. Overall the surgeons provided useful feedback on the pilot version for the delivery experiment and provided great insight into the effectiveness of the model and the improvements for future models.

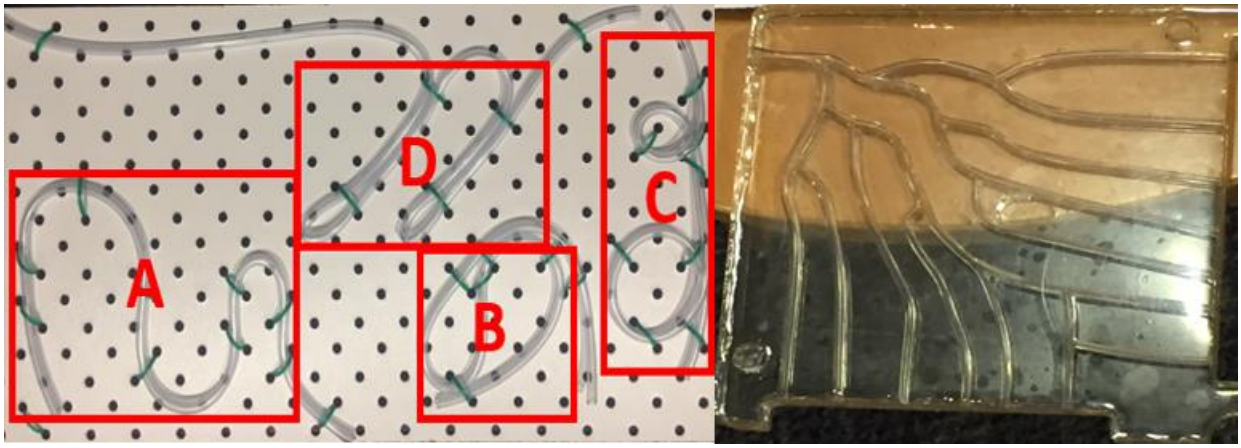

Figure 36: LHS system setup in sections, RHS a stent delivery system in solid gel

There was reasonable progress for the deliverability project, showing potential improvements for the future to provide meaningful results for stents clinically. The compression study only progressed to creating an experimental protocol. This study on the compressive strength of commercial stents would be highly valuable to further validate the current computational simulations. In addition, this study will provide up-to-date bench testing results of commonly used stents, which has not been done in the past 5-10 years. Nonetheless, both these experimental studies will provide useful data to further validate computational models and provide clinically relevant data on commercial stents mechanical performance.

The static structural analysis on stents has been well evaluated in this study, generating computational simulations for longitudinal compression, flexibility and radial strength. Each simulation captures a different mechanical aspect, which should be evaluated for stent designs. The longitudinal compression and flexibility focus predominantly on connecter type and alignment compared to the radial strength test which investigates the stent ring strength. These validated simulations can further assist with stent design verification and can be used in conjunction with other stent studies to validate performance. Some of the findings from the study may not be directly translatable to clinical practice, for example the stents were analysed in a simplified environment and thus do not account for patient specific geometries and conditions that could further impact stent performance.

Furthermore, the concept of optimal stent designs can be generated using the current computational simulations and multi-object optimisation strategy. A study focusing on mechanical performance can investigate these three objectives through the simulations by altering the variables for the stent geometric parameters. This will create a large variety of stent structures which can be analysed mechanically. Future studies should also involve other aspects in the optimisation process, such as haemodynamic flow and material to artery ratio. The optimisation method aims to develop ideal stent geometries and provide a better understanding of mechanical and flow performance of stents in vessels. To truly evaluate and optimise for patient specific conditions, the use of magnetic resonance imaging would provide a better understanding of the patient's vessel geometry and stent operational environment. Although this method would provide ideal stents for patient specific conditions, it is not a marketable opportunity for commercial suppliers due to the large examination costs. Overall, this study provided analysis on the mechanical performance of stents, which can be used to improve key characteristics of stents such as structural stability and flexibility for a more thorough stent investigation.

Chapter 6 – Conclusion

This thesis has attempted to further develop the understanding of mechanical performance of coronary stents under different loading and delivery conditions. This approach was conducted computationally using the commercial software ANSYS workbench and experimentally through bench testing. There was three mechanical studies constructed, computationally testing different aspects of the stent structure and two bench tests designed. The computational studies evaluated compressive strength, stent flexibility and radial strength. The experiments in this study focused on bench testing stents for compression and deliverability.

The stent geometries used seven design variables to influence the stent structures, which were originally optimised for hemodynamic flow. After performing a mechanical assessment of the 18 non-dominant solutions from the hemodynamic study, certain geometric characteristics became important in terms of mechanical performance. Stents that had one connector may have good hemodynamic flow properties but will consistently fail mechanically. The study determined multiple connectors between rings and straight connector demonstrated a superior compressive stiffness. Majority of the stents showed a considerably weaker compressive stiffness (<0.05 N/mm) and bending stiffness (0.074-1.86 N/mm^2) compared to commercial stents compressive (0.16-0.53 N/mm) and bending stiffness's (0.62-8.65 N/mm^2). A material study was conducted using the constructed computational studies and found that the best materials to use would be platinum chromium, cobalt chromium or stainless steel as magnesium is considered to be too weak of a material and may fail more often.

The experimental studies are in the preliminary phases but have proven that their conceptual design can effectively test the mechanical performance and that the results from the studies can provide clinically relevant data for stent improvement. The surgeons believe that the delivery model pathway accurately displays obstacles that would occur on the delivery of a stent through a vessel, which can be useful in understanding the mechanics involved in the procedures.

By considering the results gathered during this project, it is evident that utilising an effective methodology, that has been validated to test different mechanical parameters has potential to reveal meaningful insights into design characteristics. Future improvements can be implements to the methodology of the computational and experimental studies to evaluate a wider range of objectives to help improve stent characteristics to reduce clinical risk and improve patient outcomes.

References

[1] J. Iqbal, J. Gunn, and P. W. Serruys, "Coronary stents: historical development, current status and future directions," *British Medical Bulletin,* vol. 106, no. 1, pp. 193-211, 2013, doi: 10.1093/bmb/ldt009.

[2] A. Fortier, V. Gullapalli, and R. A. Mirshams, "Review of biomechanical studies of arteries and their effect on stent performance," *IJC Heart & Vessels,* vol. 4, pp. 12-18, 2014/09/01/ 2014, doi: https://doi.org/10.1016/j.ijchv.2014.04.007.

[3] A. Q. Y. Fu, "Research of Numerical Simulation of Biomechanics on In-stent-restenosis," *Journal of Vascular Medicine & Surgery,* vol. 03, no. 01, 2015, doi: 10.4172/2329-6925.1000181.

[4] T. J. Gundert, "Improving Cardiovascular Stent Design Using Patient-Specific Models and Shape Optimization," *Conference Proceedings*

2011.

[5] M. Farhan Khan, *Design optimisation for stent manufacture*. 2018.

[6] T. Watson, M. W. I. Webster, J. A. Ormiston, P. N. Ruygrok, and J. T. Stewart, "Long and short of optimal stent design," *Open Heart,* vol. 4, no. 2, p. e000680, 2017, doi: 10.1136/openhrt-2017-000680.

[7] A. Schiavone, "Computational modelling of stent deployment and mechanical performance inside human atherosclerotic arteries," *Conference Proceedings,* 2015.

[8] H. Yang, "Study of Mechanical Performance of Stent Implants Using Theoretical and Numerical Approach," *Conference Proceedings,* 2015.

[9] F. Fogarotto, "Finite Element Analysis of Coronary Artery Stenting," *Conference Proceedings,* 2010.

[10] M. Ferraro, "Advanced Modeling of Stents: from constitutive modeling to biomedical (isogeometric) analysis," 2014.

[11] N. Pal, J. Din, and P. O'Kane, *Contemporary Management of Stent Failure: Part One*. 2019, p. 10.

[12] R. L Noad, C. G Hanratty, and S. Walsh, *Clinical Impact of Stent Design*. 2014, pp. 89-93.

[13] K. Iwasaki *et al.*, "Flexibility and Stent Fracture Potentials Against Cyclically Bending Coronary Artery Motions: Comparison Between 2-Link and 3-Link DESs," *The American Journal of Cardiology,* vol. 111, no. 7, Supplement, p. 26B, 2013/04/02/ 2013, doi: https://doi.org/10.1016/j.amjcard.2013.01.355.

[14] J. A. Ormiston *et al.*, "Stent longitudinal flexibility: A comparison of 13 stent designs before and after balloon expansion," *Catheterization and Cardiovascular Interventions,* vol. 50, no. 1, pp. 120-124, 2000, doi: 10.1002/(SICI)1522-726X(200005)50:1<120::AID-CCD26>3.0.CO

2-T.

[15] T. Hiromasa *et al.*, "INCIDENCE AND CLINICAL IMPACT OF LONGITUDINAL STENT DEFORMATION AFTER THE PROMUS ELEMENT PLATINUM CHROMIUM-EVEROLIMUS ELUTING STENT IMPLANTATION," *Journal of the American College of Cardiology,* vol. 69, no. 11, Supplement, p. 1374, 2017/03/21/ 2017, doi: https://doi.org/10.1016/S0735-1097(17)34763-0.

[16] M. Pitney *et al.*, "Major stent deformation/pseudofracture of 7 Crown Endeavor/Micro Driver stent platform: incidence and causative factors," (in eng), *EuroIntervention,* vol. 7, no. 2, pp. 256-62, Jun 2011, doi: 10.4244/eijv7i2a41.

[17] P. D. Williams *et al.*, "Longitudinal stent deformation: a retrospective analysis of frequency and mechanisms," (in eng), *EuroIntervention,* vol. 8, no. 2, pp. 267-74, Jun 20 2012, doi: 10.4244/eijv8i2a41.

[18] J. A. Ormiston, B. Webber, B. Ubod, J. White, and M. W. Webster, "Stent longitudinal strength assessed using point compression: insights from a second-generation, clinically related bench

test," (in eng), *Circ Cardiovasc Interv,* vol. 7, no. 1, pp. 62-9, Feb 2014, doi: 10.1161/circinterventions.113.000621.

[19] "Patents

"Intravascular Stent" in Patent Application Approval Process (USPTO 20160045345)," ed. Atlanta, 2016, p. 5505.

[20] R. C. Hibbeler and V. Sekar, *Mechanics of Materials*. 2013.

[21] K. Nisbett and R. G. Budynas, *Shigley's Mechanical Engineering Design, 10th Edition*. 2015.

[22] A. Kastrati *et al.*, "Intracoronary Stenting and Angiographic Results," *Circulation,* vol. 103, no. 23, pp. 2816-2821, 2001, doi: doi:10.1161/01.CIR.103.23.2816.

[23] X. Shen, Z. Min Xie, Y. Quan Deng, and S. Ji, "Effects of Metal Material Stent Design Parameters on Longitudinal Stent Strength," *Key Engineering Materials,* vol. 723, pp. 299-304, 12/01 2016, doi: 10.4028/www.scientific.net/KEM.723.299.

[24] N. Paryab, D. S. Cronin, and P. Lee-Sullivan, "Finite element methods to analyze helical stent expansion," *International Journal for Numerical Methods in Biomedical Engineering,* vol. 30, no. 3, pp. 339-352, 2014, doi: 10.1002/cnm.2605.

[25] N. Rebelo, R. Radford, A. Zipse, M. Schlun, and G. Dreher, "On Modeling Assumptions in Finite Element Analysis of Stents," *J. Med. Devices,* vol. 5, no. 3, 2011, doi: 10.1115/1.4004654.

[26] N. Lebaal, M. Azaouzi, and S. Roth, "Shape optimization of coronary stents based on Finite Element Analysis," *Computer Methods in Biomechanics and Biomedical Engineering,* vol. 20, no. sup1, pp. 119-120, 2017, doi: 10.1080/10255842.2017.1382888.

[27] Q. Wang, G. Fang, Y. Zhao, G. Wang, and T. Cai, "Computational and experimental investigation into mechanical performances of Poly-L-Lactide Acid (PLLA) coronary stents," *Journal of the Mechanical Behavior of Biomedical Materials,* vol. 65, pp. 415-427, 2017/01/01/ 2017, doi: https://doi.org/10.1016/j.jmbbm.2016.08.033.

[28] I. Menown, R. Noad, E. Garcia, and P. I. Meredith Am, "The Platinum Chromium Element Stent Platform: from Alloy, to Design, to Clinical Practice," *Advances in therapy,* vol. 27, pp. 129-41, 03/01 2010, doi: 10.1007/s12325-010-0022-9.

[29] A. Idziak-Jabłońska, K. Karczewska, and O. Kuberska, "Modeling of mechanical phenomena in the platinum-chromium coronary stents," *Journal of Applied Mathematics and Computational Mechanics,* vol. 16, pp. 29-36, 12/01 2017, doi: 10.17512/jamcm.2017.4.03.

[30] T. R. Choudhury *et al.*, "Longitudinal deformation bench testing using a coronary artery model: a new standard?," *Open Heart,* vol. 4, no. 2, p. e000537, 2017, doi: 10.1136/openhrt-2016-000537.

[31] G. Leibundgut *et al.*, "Longitudinal compression of the platinum-chromium everolimus-eluting stent during coronary implantation: predisposing mechanical properties, incidence, and predictors in a large patient cohort," *Catheterization and cardiovascular interventions : official journal of the Society for Cardiac Angiography & Interventions,* vol. 81, no. 5, p. E206, 2013, doi: 10.1002/ccd.24472.

[32] Q. Wang, G. Fang, Y.-H. Zhao, and J. Zhou, "Improvement of Mechanical Performance of Bioresorbable Magnesium Alloy Coronary Artery Stents through Stent Pattern Redesign," *Applied Sciences,* vol. 8, no. 12, 2018, doi: 10.3390/app8122461.

[33] T. Yokoo *et al.*, "Development of Test Methods for Mechanical Property Evaluation of Balloon-Expandable CoCr Alloy Stent," *Journal of the Japanese Society for Experimental Mechanics,* vol. 14, no. Special_Issue, pp. s285-s290, 2014, doi: 10.11395/jjsem.14.s285.

[34] A. Kumar, R. Ahuja, P. Bhati, P. Vashisth, and N. Bhatnagar, "Design Methodology of a Balloon Expandable Polymeric Stent," *Journal of Biomedical Engineering and Medical Devices,* vol. 04, 01/01 2019, doi: 10.35248/2475-7586.19.4.139.

[35] "What is Hooke's Law?" https://www.khanacademy.org/science/physics/work-and-energy/hookes-law/a/what-is-hookes-law (accessed 4/5/2020, 2020).
[36] "Hooke's Law." http://labman.phys.utk.edu/phys221core/modules/m3/Hooke's%20law.html (accessed 4/5/2020, 2020).
[37] P. Szabadits and J. Dobranszky, "Trackability and Flexibility of Coronary Stents," *Materials Science Forum,* vol. 659, pp. 337-342, 09/01 2010, doi: 10.4028/www.scientific.net/MSF.659.337.
[38] "Young's Modulus Formula." https://www.toppr.com/guides/physics-formulas/youngs-modulus-formula/ (accessed 4/5/2020, 2020).
[39] S. N. Kumar, "Design and Structural Analysis of Skid Landing Gear," *International Journal of Current Engineering and Technology,* vol. 2, pp. 635-642, 01/01 2013, doi: 10.14741/ijcet/spl.2.2014.121.
[40] "AISI Type 304 Stainless Steel." http://asm.matweb.com/search/SpecificMaterial.asp?bassnum=mq304a (accessed 20/4/2020, 2020).
[41] "Cobalt Chromium Alloy." https://www.americanelements.com/cobalt-chromium-alloy (accessed 20/4/2020, 2020).

Appendix A – Delivery Experiment

Table 8: Delivery Experiment radius of curvature at each junction

DELIVERY POINT	CURVATURE (MM)
A	30
B	20
C	10
D	Varying
E	Varying
F	20
G	7.5
H	Varying (small)

Appendix B – Deliverability Experiment Questionnaire

Score 1-5 (least favourable to most favourable)

Questions	Score (1-5)	Comments
Difficulty level manoeuvring section A?		
Difficulty level manoeuvring section B?		
Difficulty level manoeuvring section C?		
Difficulty level manoeuvring section D?		
Difficulty level manoeuvring section E?		
Difficulty level manoeuvring section F?		
Difficulty level manoeuvring section G?		
Difficulty level manoeuvring section H?		
Tubular pathway accurately represented potential vascular situations compared to live patient?		
Manipulation of the guidewire and catheter was realistic in the model compared to live patient?		
Manipulation of the guidewire and catheter was realistic in the model compared to virtual simulator?		
I believe the model could be useful tool for training basic endovascular guidewire handing skills		
I feel that my catheter and guidewire handling skills could improve by training on this model		
What vascular situations could be added?		
Do you feel this model accurately displays the delivery of a stent through a vessel?		
What other improvements do you believe can be made to the model?		

Appendix C – Commercial Stents Comparison

This sections includes tables used when comparing simulated results with commercial products.

Table 9: Compressive stiffness commercial stent comparison

Type	**Cypher Select**	**Liberte**	**Vision Xience V**	**Multilink 8 Xience Prime**	**Driver Endeavour**	**Integrity Resolute**	**Omega Promus Element**
Material	Stainless steel	Stainless steel	Cobalt Chromium	Cobalt Chromium	Cobalt Chromium	Cobalt Chromium	Platinum Chromium
Thickness (µm)	140	100	81	81	91	91	81
Connector Number	6	3	3	3	2	2	2
Compressive stiffness (N/mm)	0.51	0.37	0.50	0.53	0.19	0.40	0.16

Table 10: Bending flexibility commercial stent comparison

Stent	**Material**	**Length (mm)**	**Diameter (mm)**	**Flexibility (Nmm^2)**	
				One-point	Four-point
Biotronik Pro-Kinetik 1	L-605	13	2.75	5.12	1.87
Biotronik Pro-Kinetik 2	L-605	22	2.84	6.09	2.15
Amazonia CroCo	L-605	12	2.5	0.62	0.23
Guidant Multi-Link Pixel RX	316-L	23	2.5	8.65	3.15
Guidant Multi-Link Zeta	316-L	15	2.78	4.18	1.52
Sanocor 1	316-L	15	2.15	1.11	0.39
Sanocor 2	316-L	11	2.78	1.11	0.39